1967

# Activation analysis of some tungsten bronzes

Margaret Ann Wechter
*Iowa State University*

# ACTIVATION ANALYSIS OF SOME TUNGSTEN BRONZES

by

Margaret Ann Wechter

A Dissertation Submitted to the
Graduate Faculty in Partial Fulfillment of
The Requirements for the Degree of
DOCTOR OF PHILOSOPHY

Major Subject: Analytical Chemistry

Approved:

Signature was redacted for privacy.

In Charge of Major Work

Signature was redacted for privacy.

Head of Major Department

Signature was redacted for privacy.

Dean of Graduate College

Iowa State University
Of Science and Technology
Ames, Iowa

1967

TABLE OF CONTENTS


| | Page |
|---|---|
| INTRODUCTION | 1 |
| Activation Analysis | 1 |
| The Tungsten Bronzes | 5 |
| THERMAL NEUTRON ACTIVATION | 12 |
| Introduction | 12 |
| Neutron Sources | 22 |
| Analysis of $Rb_xWO_3$ | 26 |
| Analysis of $La_xWO_3$ | 32 |
| Analysis of $Ho_xWO_3$ | 35 |
| Analysis of $U_xWO_3$ | 38 |
| ACTIVATION WITH 14 Mev NEUTRONS | 42 |
| Introduction | 42 |
| Neutron Source | 43 |
| Analysis of $Ba_xWO_3$ | 43 |
| HIGH ENERGY PHOTON ACTIVATION | 50 |
| Introduction | 50 |
| Irradiation Source | 50 |
| Analysis of $K_xWO_3$ | 60 |
| Analysis of $Gd_xWO_3$ and $Eu_xWO_3$ | 63 |
| RELATIONS BETWEEN X VALUE AND LATTICE PARAMETER | 71 |
| SUMMARY | 74 |
| LITERATURE CITED | 76 |
| ACKNOWLEDGMENTS | 79 |

# INTRODUCTION

## Activation Analysis

Activation analysis depends only upon the nuclear properties of elements, and thus differs basically from other analytical methods which depend on the chemical and/or physical states of elements. Activation itself involves the transformation of a stable nucleus to a radionuclide by irradiation with photons or particles possessing sufficient energy to induce a transformation. The most common irradiation source for activation analysis is the nuclear reactor which affords an intense source of thermal neutrons. Most nuclei irradiated in this manner undergo the neutron capture, or $(n,\gamma)$ reaction, which serves to increase the atomic mass by one unit and generally leads to the formation of a radionuclide. Other irradiation sources for activation analysis are particle accelerators which provide high intensity sources of x-rays, fast neutrons, protons, deuterons and other charged particles.

The first experiment in activation analysis was performed in 1936 by von Hevesy and Levi, (1) who used a Ra-Be neutron source to determine the amount of dysprosium present in a rare earth matrix. Seaborg and Livengood, (2) in 1938, initiated activation analysis in the United States by determining trace quantities of gallium in extremely pure iron by bombardment with cyclotron produced deuterons. In 1939, von Halban, Joliot and Kowarski (3) discovered that neutrons are produced in the fission of heavy nuclei, a fact which led to the nuclear reactor, used extensively in activation analysis. Since these early beginnings, the state of the art has progressed quite rapidly. Many of the widespread applications of activation analysis have been summarized in a number of review articles

and bibliographies (4-14) which have appeared in the literature during the last decade.

For the production of a radionuclide by a single reaction in the constant flux of a nuclear reactor or other irradiation facility for which cross section and flux data are available, the rate of accumulation of a radionuclide is given by the difference between its rates of production and decay.

$$\frac{dN^1}{dt} = P - \lambda N^1 \qquad (1)$$

The rate of production, P, is expressed as $N\sigma\phi$, in which N represents the number of target atoms, $\sigma$ the cross section in $cm^2$, and $\phi$ the flux of incident particles per $cm^2$ per second. In the irradiations for the purpose of analysis, any change in N during irradiation is completely negligible. The rate of decay of a radionuclide is expressed by $\lambda N^1$, where $\lambda$ represents the decay constant and N the number of atoms of product nuclide. If radioactive decay is the only important method of removal of activated species, equation 1 is valid. However, if the product nuclide has a high neutron cross section, its removal by the process of secondary neutron capture must be considered.

Assuming that N remains constant during irradiation and that radioactive decay is the only method of removal of the activated species, the solution to equation 1 is

$$N^o = \frac{N\sigma\phi}{\lambda}(1-e^{-\lambda t_1}) \qquad (2)$$

in which $t_1$ is the duration of irradiation. At any time, $t_2$, after irradiation, the activity of the irradiated species is given by

$$A = \lambda N^1 = N\sigma\phi(1-e^{-\lambda t_1})e^{-\lambda t_2}, \qquad (3)$$

or, if N is replaced by $\frac{WN_A f}{M}$, in which W corresponds to the weight of

element present, $N_A$ to Avogadro's number, f to the fractional isotopic abundance of the target nuclei, and M to the atomic weight of the element, equation 3 becomes

$$A = \lambda N^1 = \frac{WN_A f \sigma \phi}{M}(1-e^{-\lambda t_1})e^{-\lambda t_2}. \qquad (4)$$

The preceding equations 3 and 4 have been derived assuming a constant particle flux. There are, however, a number of factors which may cause variations in the flux, the most notable of which is the flux perturbation arising from absorption in the sample, commonly known as self-shielding. The self-shielding effect may result from activation with any kind of particle, and is a function of the absorption cross section which may differ considerably from the activation cross section (15). In general, samples exhibiting the self-shielding effect posses rather large cross-sections, so that the flux is attenuated inward from the surface of the sample. Thus, there is a high probability that the incoming particles will be strongly absorbed in the outer layers of the sample. This absorption results in a flux gradient which reaches a minimum value at the center of the sample. (16)

The problem of self-shielding must be considered in most activation analysis experiments. Several experimental methods for eliminating self-shielding have been proposed. The first of these methods involves the irradiation of samples which vary in weight, but not in composition. After irradiation a graph of specific activity versus sample weight is made, and from this it is possible to determine the maximum weight of sample which can be irradiated without introducing a measurable self-shielding error. Thereafter, all irradiated samples should be limited to this size. It is essential in this type of determination that sample geometry remain constant, and that one sample of very small weight be irradiated in order that the

graph may be extrapolated to the zero weight value.

A technique suggested as a means to eliminate significant self-shielding effects involves dilution of the sample by mixing it with an inert matrix; a substance which exhibits little or no self-shielding. Extreme care must be taken to insure homogeneity, however, and thus this method must be limited to materials of small particle size. It is possible to assure homogeneity by dissolution in water.

One of the chief disadvantages of the preceding two methods is that reagent blanks must be used in both cases. Thus, one of the principal advantages of activation analysis is eliminated.

Another method proposed for the elimination of self-shielding effects is the internal standard technique. This process involves the preparation of a homogeneous mixture of a known quantity of the element to be determined and a quantity of the sample being analyzed. The mixture serves as a reference standard and is irradiated together with, and under the same conditions as, the sample. This technique also suffers from the disadvantage that the sample mixture must be homogeneous in order that valid results might be achieved. It does, however, eliminate the necessity for the inert matrix referred to above, since the sample and standard are similar in composition.

A comparison method is probably used most often, in which the activity produced in a standard sample of known weight is compared to that produced in an unknown sample. Thus, the equation

$$\frac{\text{Activity of Standard}}{\text{Weight of Standard}} = \frac{\text{Activity of Unknown}}{\text{Weight of Unknown}} \qquad (5)$$

may be solved for the unknown quantity to give the weight of element present in the sample. For this method it is necessary that standard and sample be of approximately the same composition if self-shielding is suspected, and that constant geometry be maintained.

In some instances more than one nuclear reaction may contribute to the formation of a given radionuclide. This is most apt to occur during bombardment with high energy particles or photons. For this case, more general mathematical expressions have been derived (17, 18) for isotopic production.

Equations 1 to 4 indicate that the sensitivity attained by activation analysis increases with increasing cross section and particle flux. Half-lives must be considered and irradiation and decay periods chosen for each situation. These are some of the more essential factors to be considered when attempting an analysis by this method. Other considerations include the irradiation sources and analyzing equipment available, and whether the analysis is to be performed destructively or nondestructively. Fortunately, the specificity of this method is high and many analyses may be performed without radiochemical separation.

## The Tungsten Bronzes

The tungsten bronzes are nonstoichiometric compounds which may be represented by the formula, $M_xWO_3$, where $0<x<1$, and M is any one of a number of elements. Wohler (19, 20) first reported the existence of the sodium tungsten bronzes in 1823, but the formula, $Na_xWO_3$, was not confirmed until 1935. (21, 22) Much of the early work in this field was concerned with the sodium tungsten bronzes. Since these early beginnings, however,

many other elements have been incorporated into tungsten bronzes, so that there is now a rather large class of compounds which corresponds to the general formula. Certain properties of these compounds, such as luster and electrical conductivity, are functions of x value. These metallic properties are largely responsible for the application of the term "bronzes" to these compounds.

Much of the interest shown in tungsten bronzes has been directed toward the sodium compounds. These have been prepared in a number of ways, beginning with Wohler's method which involved the hydrogen reduction of a sodium tungstate melt. A more sophisticated method of preparation is the growth of single crystals from cathodic reduction of a sodium tungstate-tungsten (VI) oxide melt. (23) Crystals have been grown with sodium x values ranging from <0.3 to nearly 1.[1] This wide variation in x has largely been responsible for the extensive interest shown in these bronzes.

A region of cubic symmetry is known for the sodium tungsten bronzes with $x>0.4$, (21, 22, 24) and a linear relation has been found to exist between the x value and lattice parameter, $a_o$, for this symmetry region. (23) Below $x = 0.4$ bronzes exist which have lower than cubic symmetry. (25, 26) The cubic sodium tungsten bronzes have been found (24) to have the perovskite structure, in which the lattice is built up of large oxygen ions whose centers occupy the corners of octahedra. Small tungsten ions, with a formal charge of +5, are located at the centers of the octahedra, while sodium ions lie between the octahedra. Obviously for $x<1$ the lattice

---

[1]Shanks, H., Ames, Iowa. Information on the sodium tungsten bronzes. Private communication. 1964.

must contain 1-x vacant interstices. There is a contraction of the lattice with decreasing sodium x value (22, 27, 28) for the following reason. In order to maintain neutrality the withdrawal of sodium must be considered as the removal of sodium atoms, not ions. The charge which it carried in the lattice must, therefore, be transferred to the tungsten, giving it a formal charge of +6 rather than +5. This increased charge on tungsten leads to a contraction in the lattice, via the reaction

$$W^{+5} + Na^{+} \text{ ----> } Na^{o} + W^{+6}. \qquad (6)$$

The lithium tungsten bronzes were first mentioned by Hallopeau (29) and Brunner, (30) who obtained dark blue to steel blue crystals by electrolysis or by reducing fused lithium paratungstate with tin. These bronzes also crystallize in cubic symmetry and assume the perovskite structure (23, 28, 31) for certain values of x. However, the x value range for the cubic form of the lithium bronzes is about 0.3 to 0.5, considerably shorter than for that in the sodium bronzes.

There are similarities between the crystal structures of the lithium and sodium tungsten bronzes, in that both crystallize with cubic symmetry in the perovskite structure. Cubic lithium bronzes, however, also differ considerably from their sodium analogs in several respects. Pure $LiWO_3$ cannot exist. The crystal lattice expands with decreasing concentration of the alkali metal, and lithium bronzes show ionic conductivity and possibly some electronic conductivity, while sodium bronzes display only electronic conductivity. (32) It has been found that the reason for these differences lies in the size of the lithium ions. The small lithium ions contract the entire lattice appreciably. Thus, expansion occurs when they are removed since, in this case, the transfer of charge to tungsten

is not sufficient to balance the charge effect of the lithium ions. Ionic conductivity is observed at temperatures as high as 450°C because the lithium ions are so small that they slip through openings in the octahedra. On the other hand, sodium ions are too large to slip through, and thus the sodium tungsten bronzes show only electronic conductivity.

The tungsten bronzes of potassium, rubidium and cesium do not crystallize in cubic symmetry. The potassium tungsten bronze displays the highest symmetry by forming tetragonal crystals, isomorphous with tetragonal $Na_xWO_3$, in the range $0.40<x<0.57$. (26, 27) In the range $0.27<x<0.31$ the $K_xWO_3$ crystals are hexagonal. (33) For their known range of x values, the rubidium (26, 34) and cesium (28) tungsten bronzes are isomorphous with hexagonal potassium tungsten bronze. Values of x for $Rb_xWO_3$ and $Cs_xWO_3$ have been reported to be within the limits $0.3<x<0.4$.

Potassium tungsten bronzes were first prepared by Laurent, (35) who reduced potassium tungstate-tungsten (VI) oxide mixtures with tin, (36) with tungsten (IV) oxide, (30) and with elemental tungsten. (26) Schaefer, (37) in 1904, first prepared $Rb_xWO_3$ by reducing rubidium carbonate-hydrogen tungstate mixtures with methane and hydrogen. Nothing was reported in the literature about $Cs_xWO_3$ until 1951, (28) when Magneli and Blomberg reported the preparation of a tungsten bronze which had the composition $Cs_{0.32}WO_3$. The preparation of this compound involved heating cesium polytungstate ($Cs_2O \cdot 4WO_3$) and tungsten (VI) oxide in vacuo at 950°C.

Conroy and Yokokawa (38) have reported the existence of a series of barium tungsten bronzes with $x<0.13$. These bronzes, the first alkaline earth tungsten bronzes to be reported in the modern literature, were prepared by the reaction of barium chloride, tungsten (IV) oxide and tungsten

(VI) oxide at 700-1000°. It has been found (38, 39) that the structure of these bronzes is isomorphous with the tetragonal I phase of $Na_xWO_3$ and $K_xWO_3$.

Tungsten bronzes of the rare earths (40) and uranium[2] have recently been reported in the literature. The initial preparation of these compounds involved the thermal reaction in vacuo of appropriate molar ratios of rare earth oxide, tungsten, and tungsten (VI) oxide. Bronzes obtained in this manner were blue violet powders. A subsequent method of preparation, electrolytic reduction of a fused mixture of rare earth tungstate and tungsten (VI) oxide at 1200°C, produced single crystals of rare earth bronzes. (41)

The range in x value varies somewhat for these bronzes, depending on the rare earth ion introduced into the lattice. An upper limit, however, appears to be reached at $<0.2$. X-ray diffraction data indicate that all these bronzes crystallize in cubic symmetry for $x = 0.1$, and that a transition from cubic to tetragonal symmetry occurs at $x \leq 0.085$.

In addition to the tungsten bronzes of the alkali metals, barium, rare earths and uranium, tungsten bronzes have been reported for copper, (42) silver, (43) and thallium. (44) It is thought that continued efforts may produce still more of these compounds.

Chemically, the tungsten bronzes are quite inert, resistive to dissolution in water and all acids. They can be oxidized by oxygen in

---

[2]Ostertag, W., Wright-Patterson A.F.B., Ohio. Information on the tungsten bronzes of uranium. Private communication. 1966.

the presence of base to tungstates, and they will reduce ammoniacal silver nitrate to silver.

Because of their lack of reactivity, the tungsten bronzes do not lend themselves well to most chemical analyses. Spitzin and Kaschtanoff (45, 46) and Magneli analyzed tungsten bronzes by converting them to the soluble tungstates, from which the metal ion concentrations could be determined by conventional means. The bronzes were decomposed by reaction with gaseous hydrogen chloride at high temperatures. Oxygen was used to oxidize the bronze to the tungstate. Raby and Banks (47) developed an analytical method based on the reactions of bromine trifluoride and hydrogen with the bronzes. Potassium and rubidium have been determined in tungsten bronzes by Sienko, (34) who put the bronzes into soluble form by fusion in a 3:1 weight mixture of sodium nitrate and sodium carbonate. The alkali metals were then determined by flame photometry.

Because of the nature of the tungsten bronzes chemical analyses require considerable time, and the samples are destroyed in all cases. Reuland and Voigt (48) have analyzed the sodium tungsten bronzes non-destructively by thermal neutron activation. Experimentally determined x values were plotted against lattice parameters for a number of cubic bronzes. The slope-intercept equation obtained was in excellent agreement with that obtained by Brown and Banks, (23) whose x values were based on the stoichiometric quantities of starting material used. Lattice parameter data were obtained from Debye-Scherrer powder photographs. In addition to the proven accuracy of this method, an added advantage lay in the fact that it was extremely rapid compared to the chemical methods.

The sodium vanadium bronzes, represented by the formula $Na_xV_2O_5$,

have also been analyzed nondestructively after irradiation with thermal neutrons. (49) Results obtained attested to the accuracy of the method and, as was true for the tungsten bronzes, the analyses were accomplished in far less time than had conventional chemical means been employed.

# THERMAL NEUTRON ACTIVATION

## Introduction

The rubidium, holmium, lanthanum and uranium tungsten bronzes were analyzed using thermal neutron activation. The nuclear properties (50, 51) of these bronzes are summarized in Tables 1 and 2.

Because of the large activation cross section of $W^{186}$, it was believed that $W^{187}$ might afford considerable interference to the gamma-ray spectra of the metal ions. Figures 1 and 2 represent gamma-ray scintillation spectra of $W^{187}$ taken using 2 different detection systems. It was found, however, that it was possible in all of the cases in question to choose gamma-rays which were well resolved from those of $W^{187}$.

Rubidium-88 was used for the analysis of rubidium. Figures 3 and 4 represent the gamma-ray scintillation spectrum of $Rb^{88}$ and of a rubidium tungsten bronze with $x = 0.4$. It can be seen that the 1.853 Mev photopeak of $Rb^{88}$ is isolated from the $W^{187}$ gamma-rays. Thus, any sample activity due to $Rb^{88}$ may be isolated from $W^{187}$ activity by scintillation spectroscopy. A consideration of their nuclear properties indicates that $Rb^{88}$ and $W^{187}$ may also be separated from each other by half-life differences.

Isolation of $Ho^{166}$ activity after the irradiation of $Ho_xWO_3$ samples was complicated by the similarity in half-lives of $Ho^{166}$ and $W^{187}$, 27 and 24 hours, and in the cross sections for the reactions which produce them. It was found, however, that $Ho^{166}$ photopeaks at 1.38 and near 1.6 Mev are free from tungsten interference. Figures 5 and 6 are the gamma-ray scintillation spectra of $Ho^{166}$ and of a $Ho_xWO_3$ sample with $x = 0.18$.

The reaction of interest for the analysis of lanthanum in $La_xWO_3$ was the thermal neutron capture by $La^{139}$ to produce 40.23 hour $La^{140}$.

Table 1. Nuclear properties of the constituents of the tungsten bronzes of rubidium, holmium and lanthanum subject to activation by thermal neutrons

| Target Nuclide | Abundance % | Cross Section (barns) | (n,γ) Reaction Product | Product Half-life | Principal gamma-rays (Mev) in order of decreasing intensity |
|---|---|---|---|---|---|
| Rb | | 0.73* | | | |
| $Rb^{85}$ | 72.15 | 0.80[a] | $Rb^{86}$ | 18.7d | 1.084 |
| $Rb^{87}$ | 27.85 | 0.12[a] | $Rb^{88}$ | 17.8m | 1.835, .899, 2.68, 1.39, 2.11, 3.24 |
| Ho | | 65* | | | |
| $Ho^{165}$ | 100.0 | 60[a] | $Ho^{166}$ | 27.2h | .081, 1.38, 1.582, 1.663, .673 |
| La | | 9.3* | | | |
| $La^{139}$ | 99.911 | 8.2[a] | $La^{140}$ | 40.23h | 1.597, .491, .323, .815, .923, .868, 2.5, .748, .434, 2.34 |
| W | | 19.2* | | | |
| $W^{180}$ | 0.135 | 30[a] | $W^{181}$ | 140d | .136, .152, .366 |

*Atomic absorption

[a]Activation

Table 1. (Continued)

| Target Nuclide | Abundance % | Cross Section (barns) | (n,γ) Reaction Product | Product Half-life | Principal gamma-rays (Mev) in order of decreasing intensity |
|---|---|---|---|---|---|
| $W^{182}$ | 26.41 | 19[a] | $W^{183m}$ | 5.5s | .060 +K-x-ray, .105, .155 |
| $W^{183}$ | 14.4 | 10.9[a] | $W^{184}$ | stable | |
| $W^{184}$ | 30.64 | 2.0[a] | $W^{185}$ | 74d | .125 |
| $W^{186}$ | 28.41 | 34[a] | $W^{187}$ | 23.8h | .686, .480, .072, .134, .618, .552, .773, .870 |
| O | | $<2 \times 10^{-4}$* | | | |
| $O^{16}$ | 99.759 | | $O^{17}$ | stable | |
| $O^{17}$ | 0.037 | | $O^{18}$ | stable | |
| $O^{18}$ | 0.2039 | $2.2 \times 10^{-4}$[a] | $O^{19}$ | 29.4s | .200, 1.37 |

Table 2. Nuclear properties of uranium subject to activation by thermal neutrons

| Target Nuclide | Abundance % | Cross Section (barns) | (n,γ) Reaction Product | Product Half-life |
|---|---|---|---|---|
| U | | 7.68* | | |
| $U^{234}$ | 0.0057 | 90[a] | $U^{235}$ | $7.1 \times 10^{8}$ y |
| | | ≤0.65[f] | | |
| $U^{235}$ | 0.714 | 107[a] | $U^{236}$, F.P.+ | $2.4 \times 10^{7}$ y |
| | | 582[f] | | |
| $U^{238}$ | 99.3 | 2.74[a] | $U^{239}$ | 23.5m |
| | | $<5 \times 10^{-4}$[f] | | |

*Atomic absorption

[a]Activation

[f]Fission

+Fission products

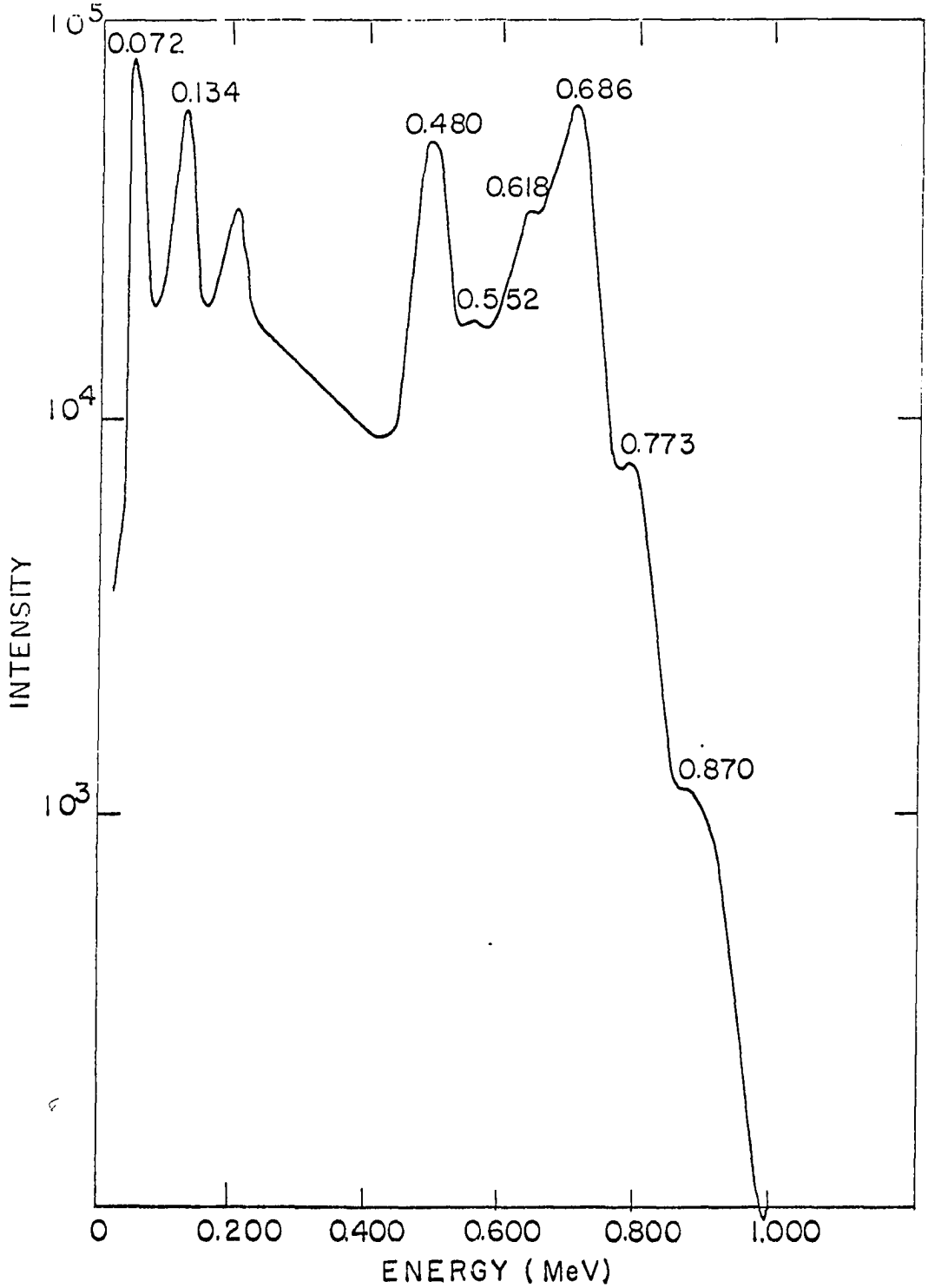


Figure 1. Gamma ray spectrum of $W^{187}$ counted in 4 x 4 inch NaI(Tl) well crystal

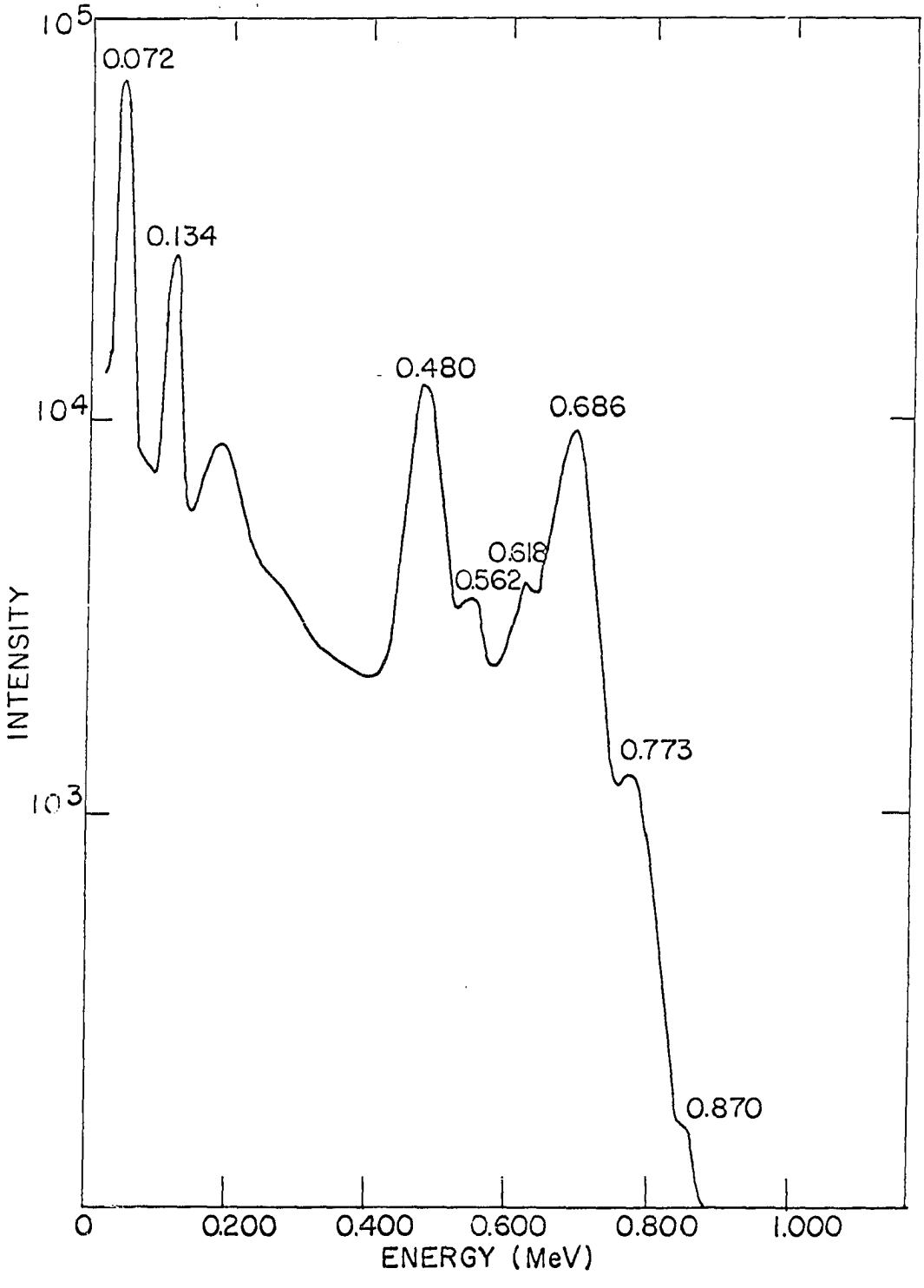


Figure 2. Gamma-ray spectrum of $W^{187}$ counted on 3 x 3 inch NaI(Tl) crystal

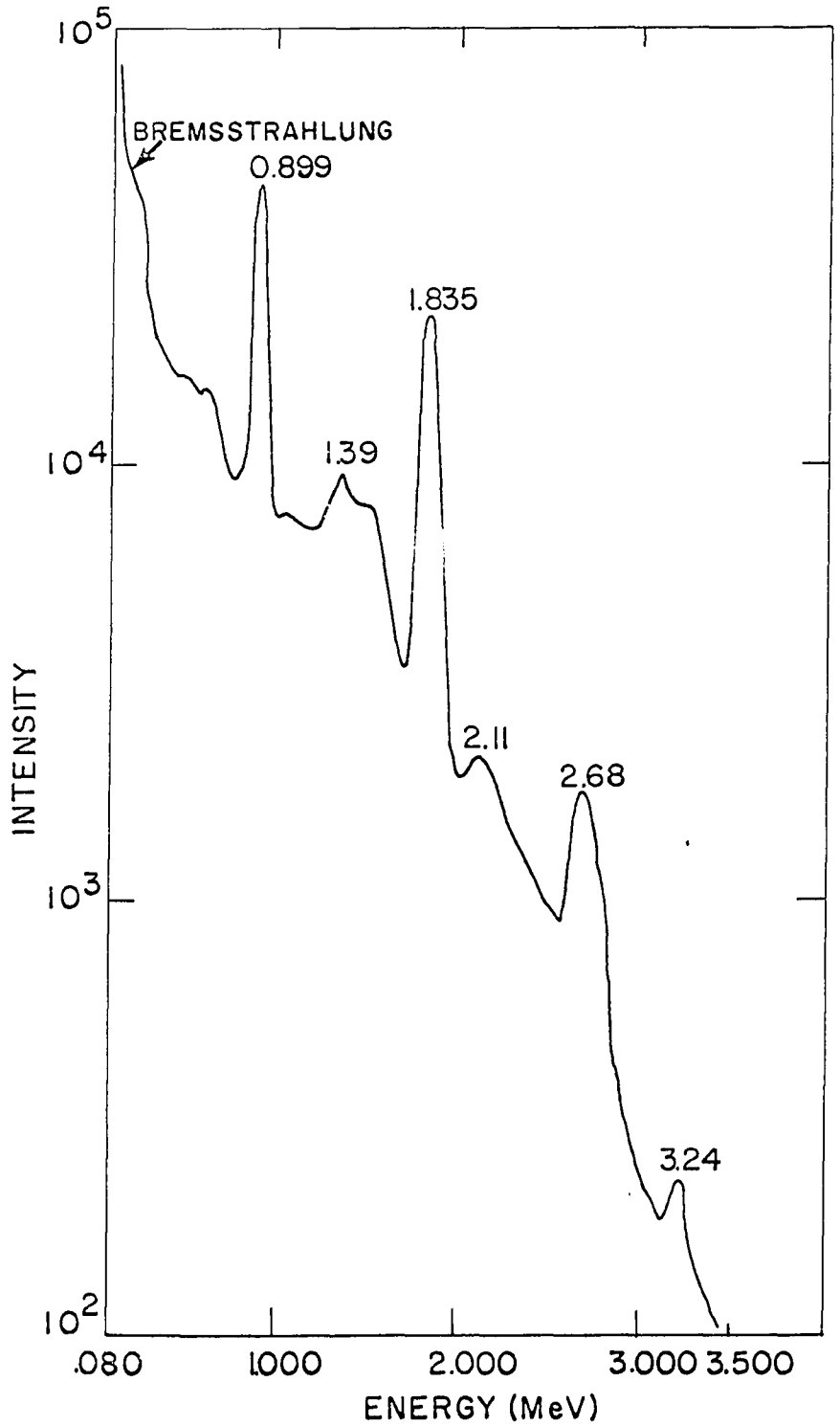


Figure 3. Gamma-ray spectrum of $Rb^{88}$

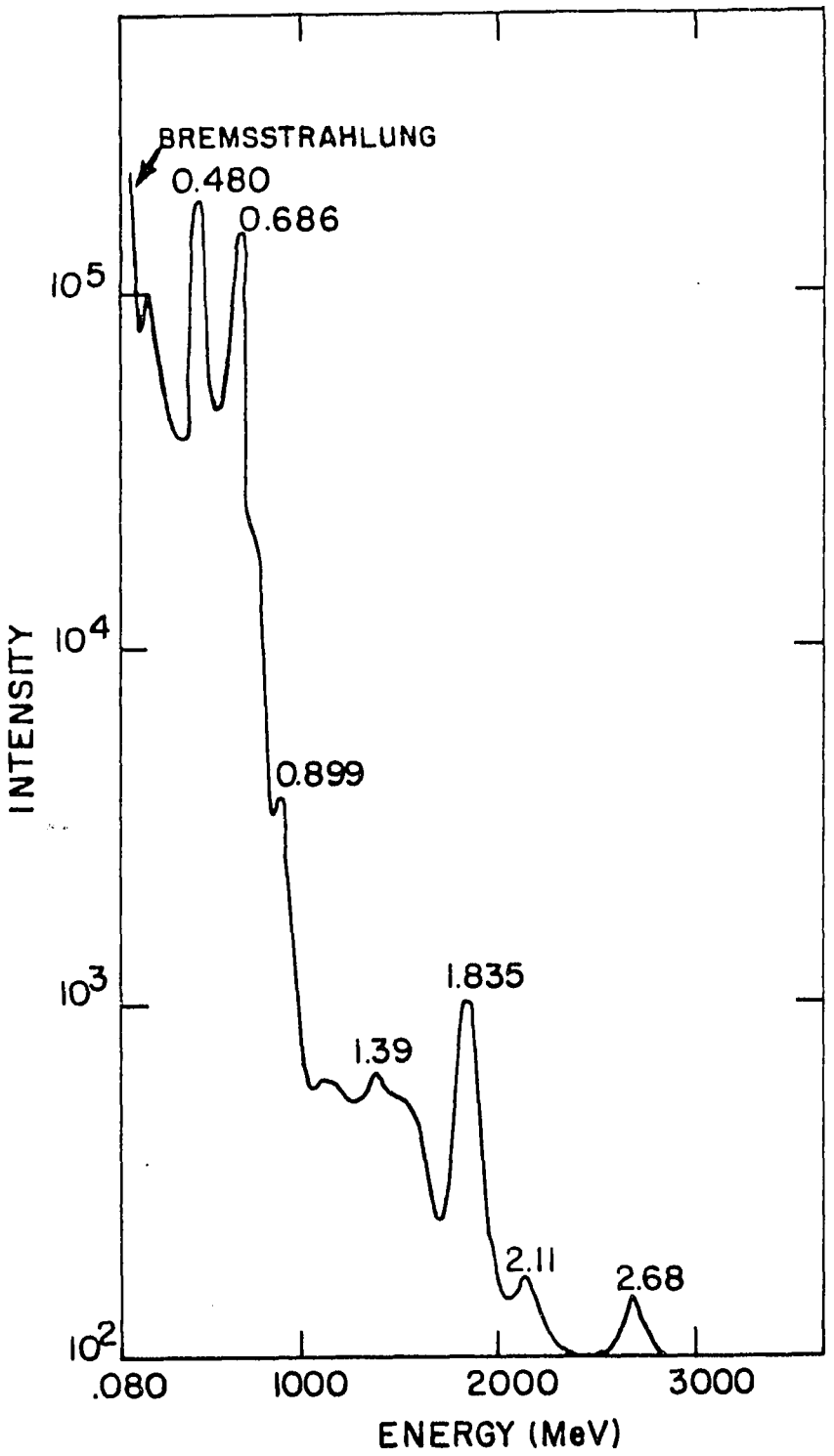


Figure 4. Gamma-ray spectrum of neutron irradiated $Rb_{0.4}WO_3$

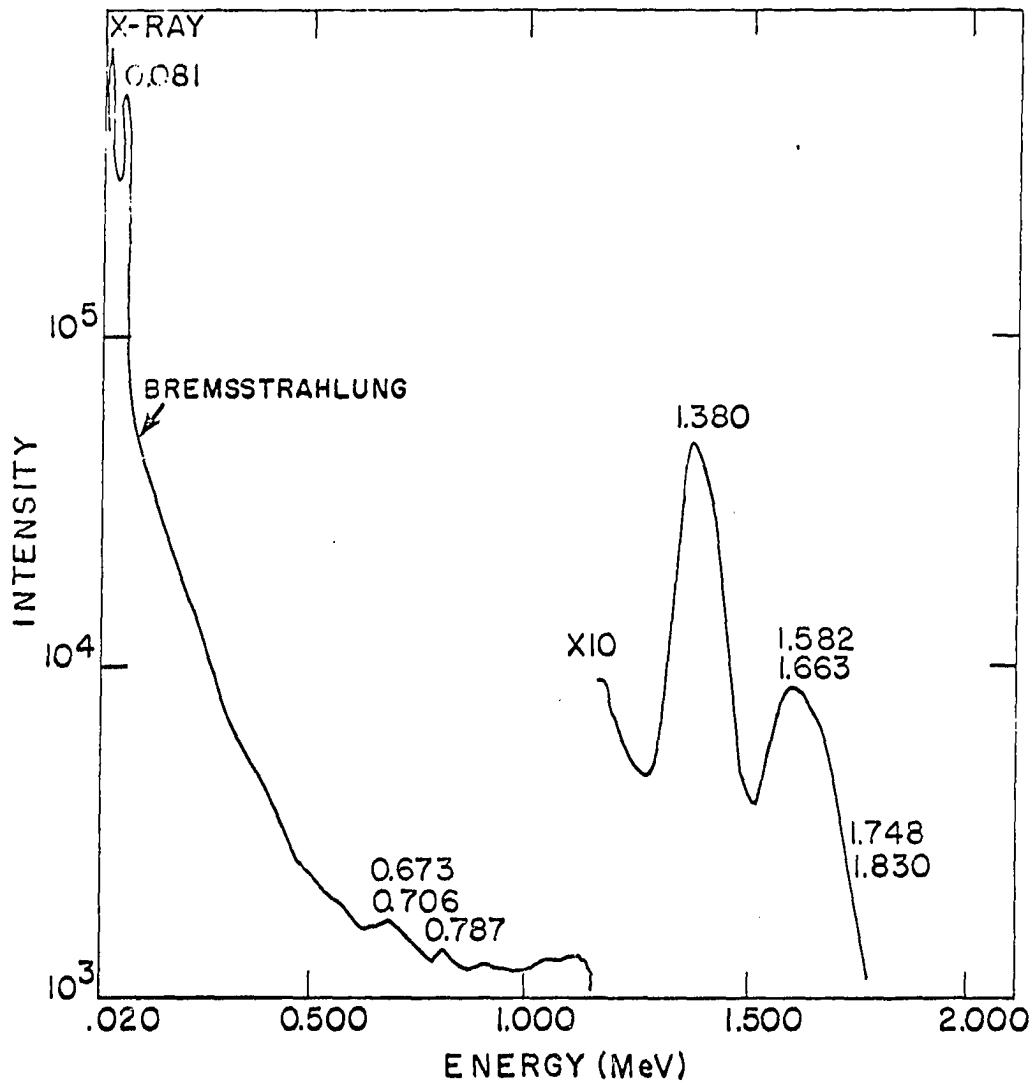


Figure 5. Gamma-ray spectrum of $Ho^{166}$

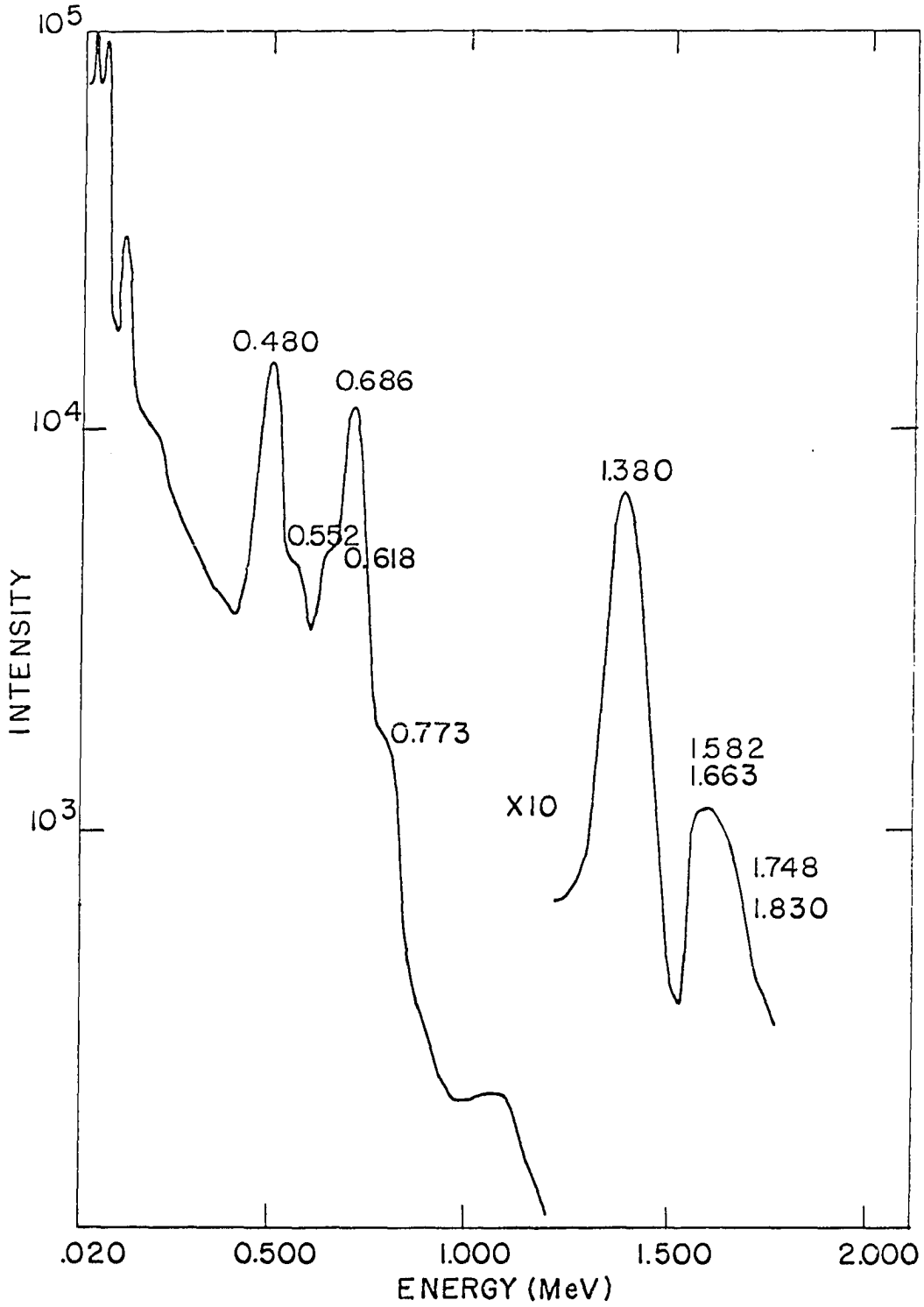


Figure 6. Gamma-ray spectrum of neutron irradiated $Ho_{0.18}WO_3$

The gamma-ray spectrum of $La^{140}$ is given in Figure 7. From Figure 8, the gamma-ray spectrum of a $La_xWO_3$ sample with x = 0.2, it can be seen that resolution of the 1.597 Mev photopeak and of the 2.09 Mev sum peak of $La^{140}$ from $W^{187}$ activity can readily be accomplished.

Irradiation of $U^{238}$ with thermal neutrons produces 23.5 minute $U^{239}$ which appeared to be a suitable radionuclide for the activation analysis of uranium. However, it was found that all gamma-rays associated with the decay of $U^{239}$ were low in energy and completely masked by gamma-rays of $W^{187}$. On the other hand, the gamma-ray spectrum of total fission products from $U^{235}$ provided a number of photopeaks which were well separated from interfering $W^{187}$ activity and suitable for counting. Figure 9 is a gamma-ray spectrum of the fission products of $U^{235}$ over the energy region of interest, accumulated 15 hours after irradiation to allow for the decay of short-lived isotopes. The gamma-ray spectrum of a $U_xWO_3$ sample with x = 0.1 is given in Figure 10. The energy region between 1.5 and 2.6 Mev, isolated from all $W^{187}$ activity, contains mainly the photopeaks of $La^{140}$, with some contribution in the peak at 1.6 Mev from 6.7 hour $I^{135}$. This region was chosen for counting. Half-life determinations indicated there was no contribution from other fission products in this region of energy and time.

## Neutron Sources

The neutron source used for the irradiations of the rubidium tungsten bronzes was the Iowa State University Training Reactor (UTR-10) operated by the Department of Nuclear Engineering. This is a 10 kilowatt reactor constructed by American-Standard and based on the "Argonaut" design of Argonne National Laboratory. It is a tank-type, heterogeneous reactor utilizing

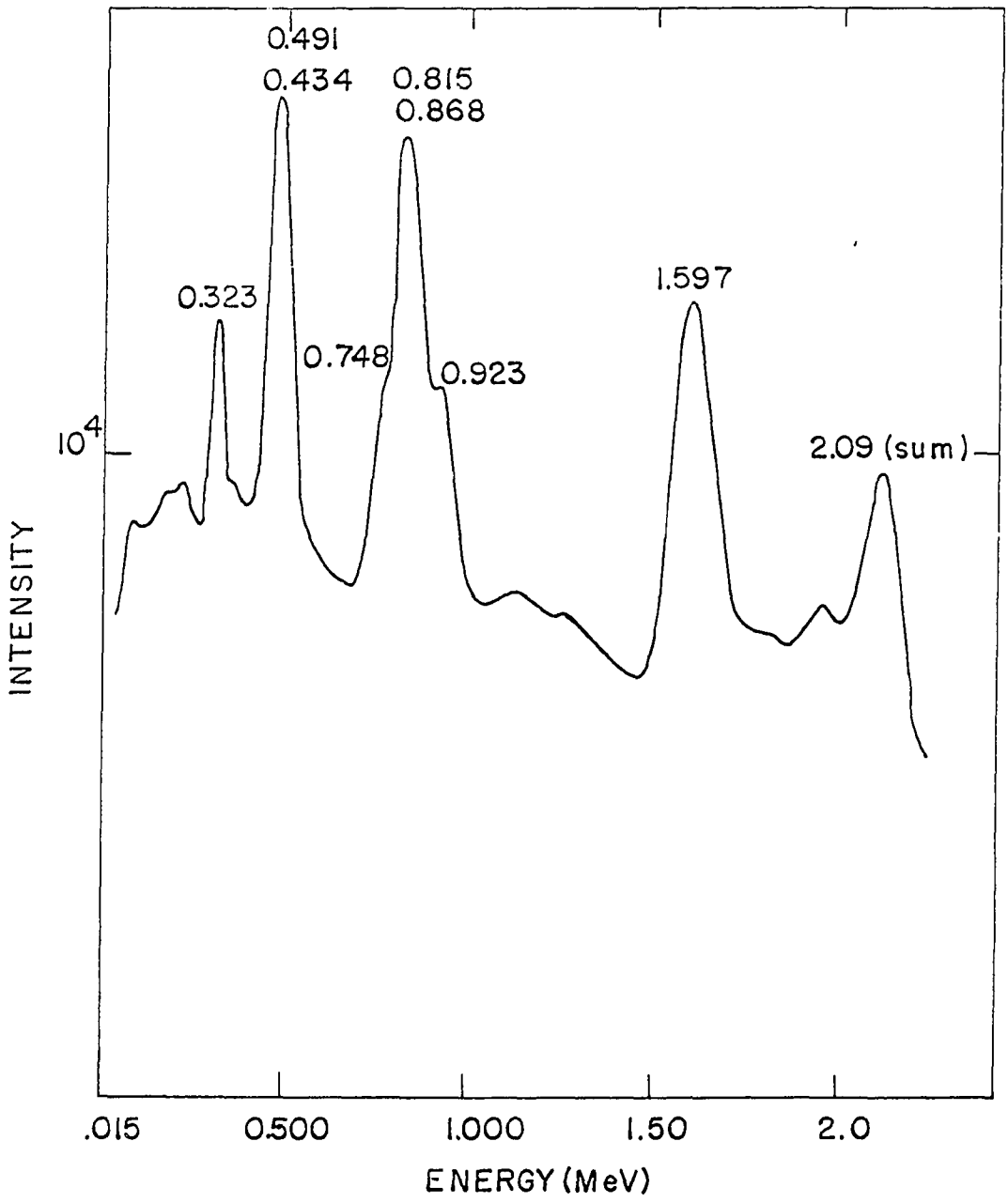


Figure 7. Gamma-ray spectrum of $La^{140}$

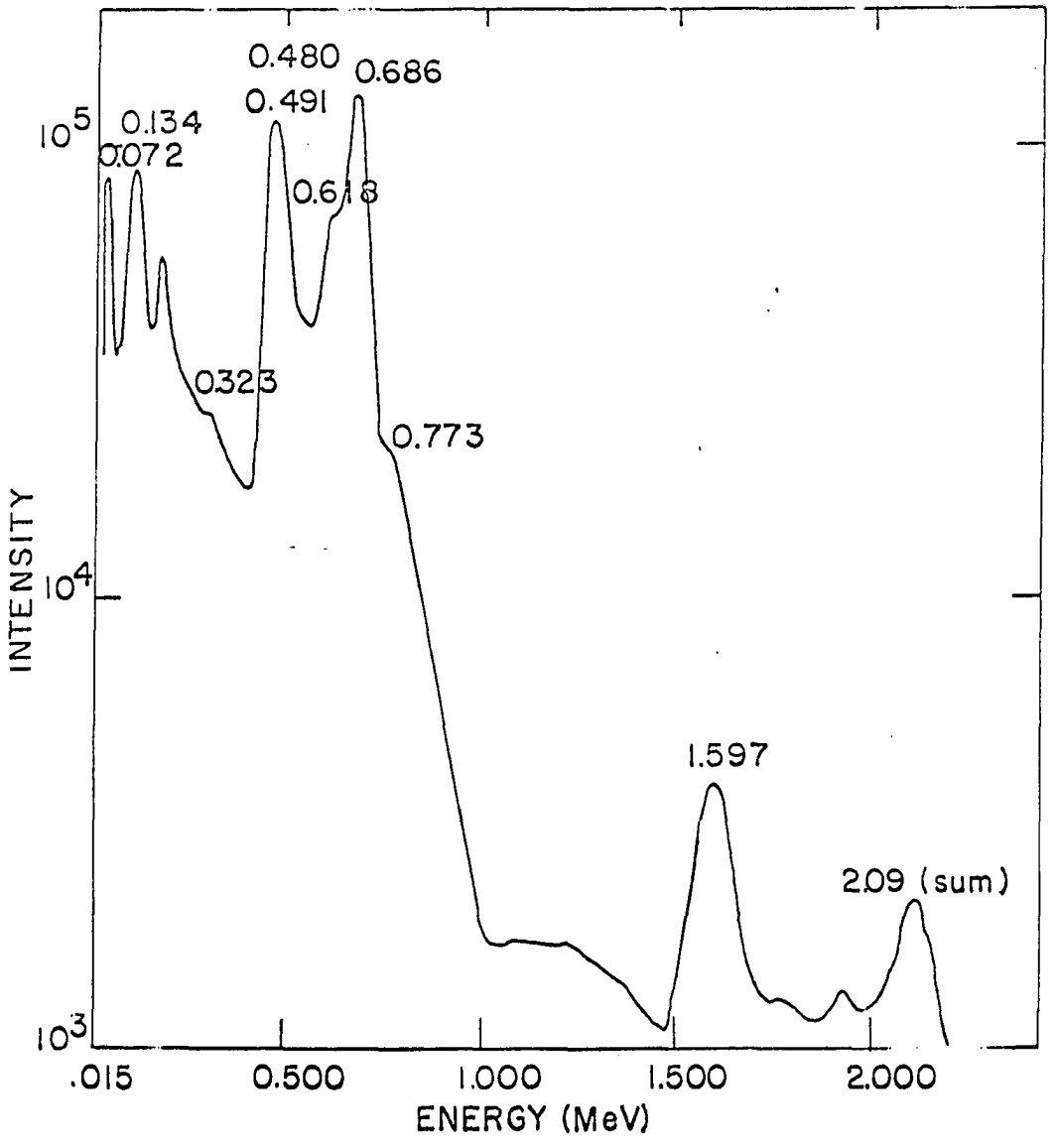


Figure 8. Gamma-ray spectrum of neutron irradiated $La_{0.2}WO_3$

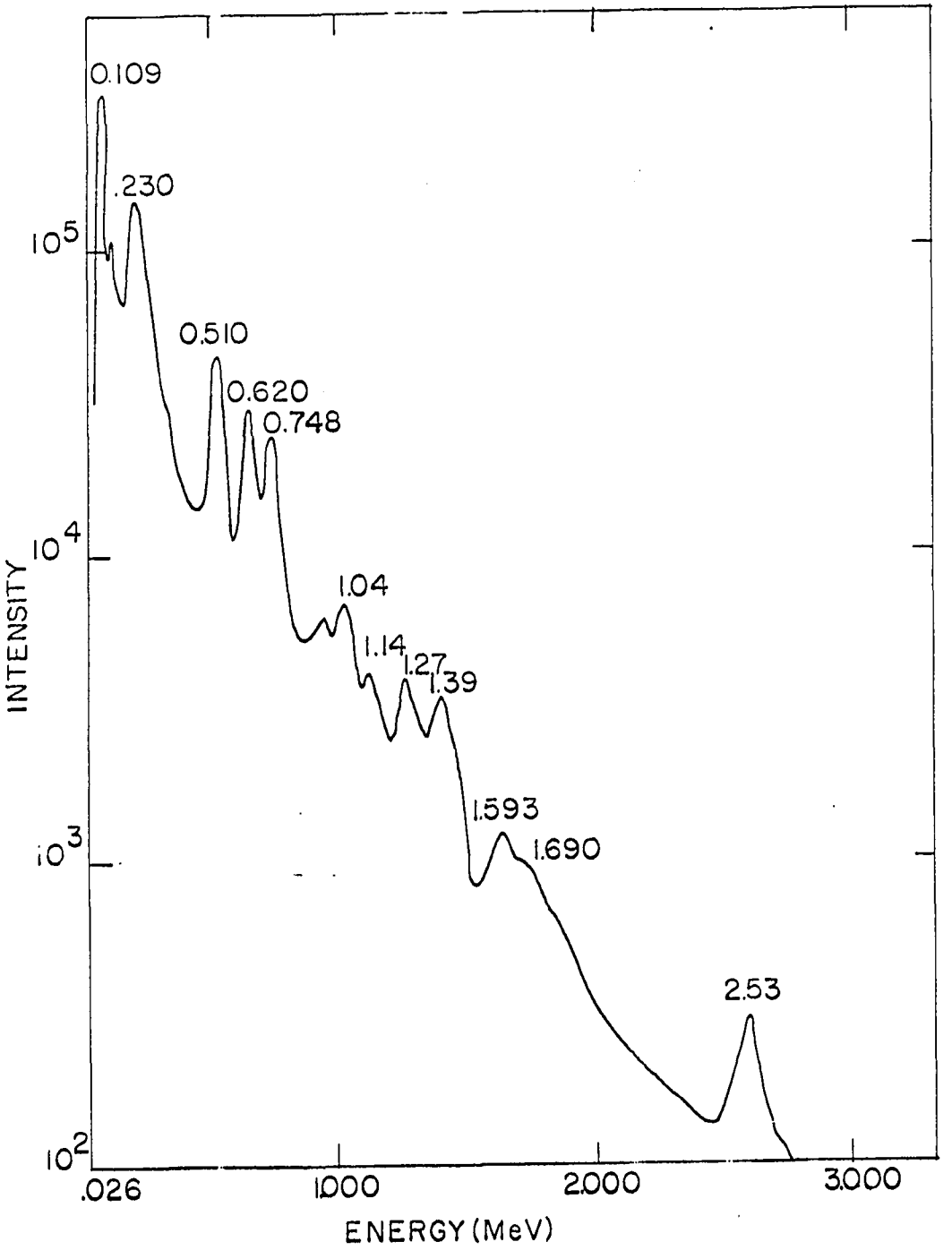


Figure 9. Gamma-ray spectrum of $U^{235}$ fission products

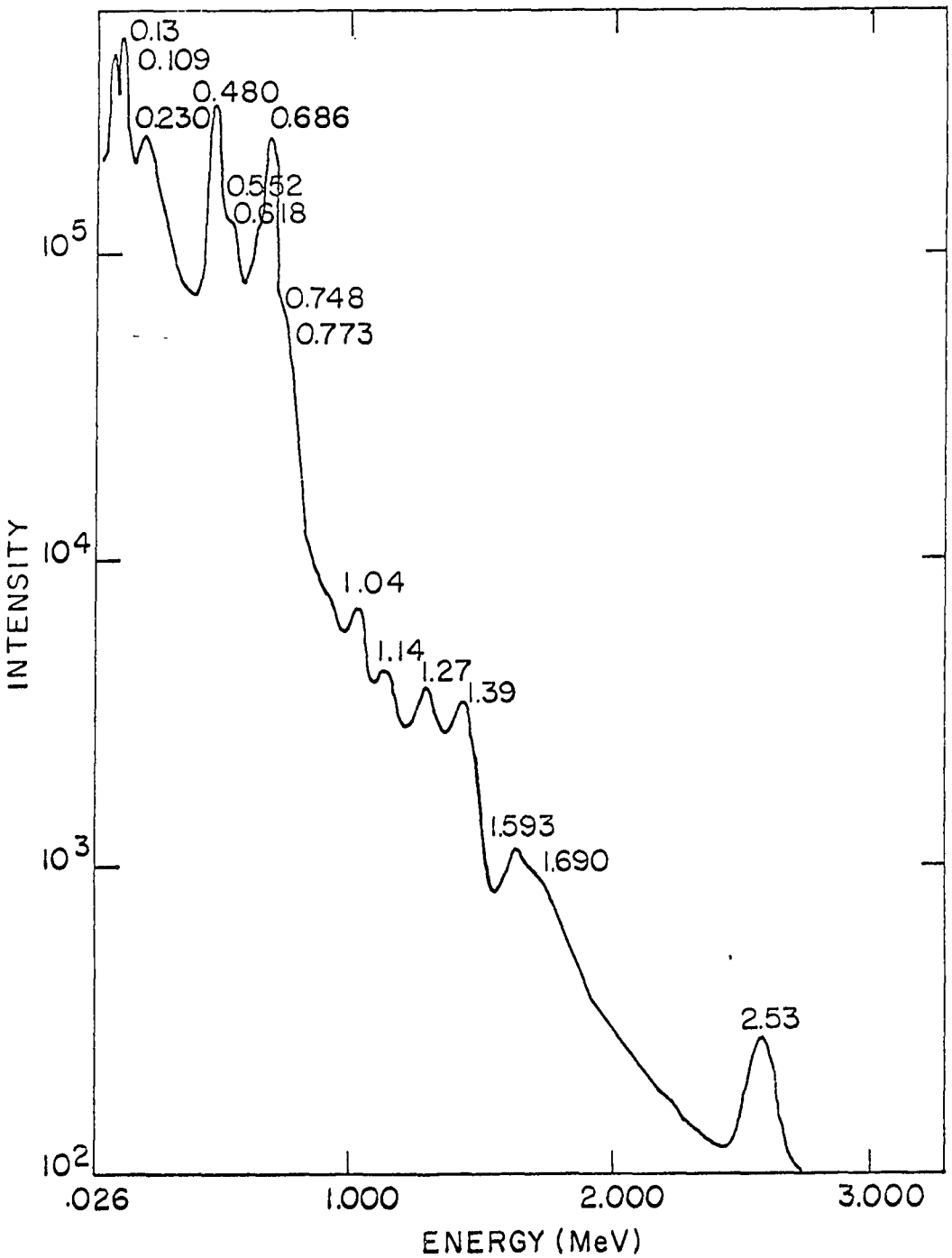


Figure 10. Gamma-ray spectrum of neutron irradiated $U_{0.10}WO_3$

light water as the coolant and graphite and light water as moderators. Access to the highest flux is achieved with a pneumatic transfer system which terminates at one of two core tanks. The pneumatic tube accomodates a "rabbit" (1 3/8 in. I. D.) which receives a thermal flux of $8 \times 10^{10}$ neutrons/$cm^2$ x sec at the maximum steady power of 10 kilowatts.

The tungsten bronzes of holmium, lanthanum and uranium were irradiated in the Ames Laboratory Research Reactor. This is a 5 megawatt reactor of the CP-5 type. It is a heterogeneous, tank-type reactor, cooled and moderated by heavy water. Two pneumatic transfer systems are used for access to high neutron flux. One of these accommodates a "rabbit" which is 2 1/2 inches in diameter. This system terminates 15 inches from the core, and at 5 megawatts the rabbit is exposed to a thermal flux of $1 \times 10^{13}$ neutrons/$cm^2$ x sec. A second pneumatic transfer system uses a "rabbit" which has a diameter of 1 inch. The system in this case terminates 6 inches from the core, exposing the rabbit to a thermal flux of $3 \times 10^{13}$ neutrons/$cm^2$ x sec at 5 megawatts.

## Analysis of $Rb_xWO_3$

The determination of rubidium concentration in $Rb_xWO_3$ was accomplished nondestructively by gamma scintillation spectrometry. The 1.835 Mev photopeak of $Rb^{88}$ was separated from $W^{187}$ interference as established by half-life considerations. A sample of the standard material, $Rb_2WO_4$, was irradiated for 30 seconds in a thermal flux of $8 \times 10^{10}$ neutrons/$cm^2$ x sec and counted with a 3 x 3 inch Harshaw NaI(Tl) crystal which was optically coupled to an RCA 8054 photomultiplier tube. Spectral data were accumulated with an RIDL Model 34-12B multichannel analyzer. The resolution, $\eta$, of

the spectrometer with this crystal, defined as

$$\eta(\%) = \frac{\text{full width at half maximum, } \Delta E, \text{ of the } Cs^{137} \text{ line} \times 100}{\text{average energy, } E \text{ (662 kev)}} \quad (7)$$

was 9.8%. Read-out was accomplished on a scaler which was attached to the analyzer. Energy discrimination was used to reject all counts except those attributable to the $Rb^{88}$ photopeak. The decay of the 1.835 Mev gamma-ray was followed through 5 half-lives, and the value found for the $Rb^{88}$ isotope, 18 minutes, agreed with the literature value (50) proving that $W^{187}$ afforded no interference to the determination of rubidium.

Samples to be analyzed were weighed on a microbalance and encapsulated for irradiation in polyethylene tubing. The encapsulated samples, together with $Rb_2WO_4$ standards, were placed in lucite holders for irradiation (Figure 11). Each holder contained 4 standards placed in positions 1, 4, 7 and 10, and generally 4 samples of each of 2 bronzes which were placed in an alternating fashion in the rest of the positions around the periphery of the holder. An empty piece of tubing, which served as a blank for the background determinations, was placed in position 13.

All samples were irradiated for 30 seconds in a thermal neutron flux of $8 \times 10^{10}$ neutrons/$cm^2$ x sec. Since tungsten has a relatively high cross section, a self-shielding determination was made. This was done by irradiating samples of $Rb_2WO_4$ which varied in weight from 1 to 25 mg. The samples were then counted and the weight of Rb present plotted against the specific activity. These data yielded a straight line with a slope of zero, which indicated that, for the sample sizes used, self-shielding was not a problem.

Following bombardment the samples and standards, which remained

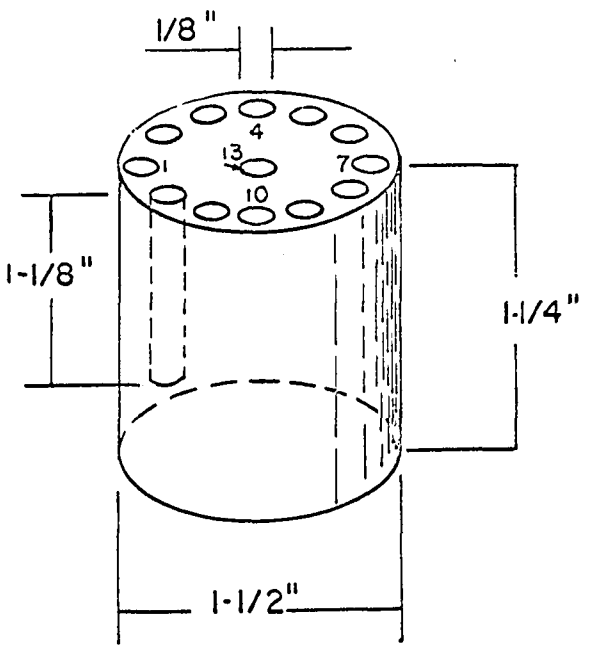


Figure 11. Sample container

encapsulated, were counted as described above. They were generally counted for total times of 1 minute, and the activities thus determined were corrected for background and decay. Counting rates were approximately 5,000-10,000 cpm so that statistical counting errors were generally on the order of 1-1 1/2%.

The rubidium x values were obtained from a comparison of the specific activities of samples and standards. Specific activities of rubidium in the standards were obtained by dividing the activities by the weights of rubidium present. The weight, W, of rubidium in each bronze sample was then obtained from the relation

$$W = \frac{A}{R}, \tag{8}$$

where A represents the $Rb^{88}$ activity of the bronze, and R the specific activity. If the oxygen to tungsten ratio is exactly 3 as it is usually assumed to be (47) the x values for the rubidium tungsten bronzes can be calculated by using the equation

$$x = \frac{\frac{F}{M_{Rb}}}{\frac{[1-F]\ 0.793}{M_W}}. \tag{9}$$

In equation 8 F represents the weight fraction of rubidium present, and $M_{Rb}$ and $M_W$ the atomic weights of rubidium and tungsten. The constant, 0.793, is the weight fraction of tungsten in $WO_3$. This formula may be generalized to include any bronze metal ion.

In order to establish the method of analysis, known mixtures of $Rb_2WO_4$ and $WO_3$ were analyzed using the above procedure. They were prepared in a ball mill which was rotated for several days. Results of these

analyses are given in Table 3.

Table 3. Thermal neutron activation analyses of known mixtures of $Rb_2WO_4$ and $WO_3$

| Sample | Standard | Milligrams of Rubidium | | x | |
|---|---|---|---|---|---|
| | | Calculated | Observed | Calculated | Found |
| Rb-1 | $Rb_2WO_4$ | 0.938 | 0.950 | 0.300 | 0.304 |
| | | 0.868 | 0.933 | | 0.325 |
| | | 0.796 | 0.838 | | 0.317 |
| | | 0.778 | 0.791 | | 0.307 |
| Av. | | | | | 0.313 ± 0.010 |
| Rb-2 | $Rb_2WO_4$ | 0.836 | 0.870 | 0.400 | 0.420 |
| | | 1.053 | 1.116 | | 0.429 |
| | | 0.775 | 0.793 | | 0.411 |
| | | 0.917 | 0.926 | | 0.403 |
| Av. | | | | | 0.416 ± 0.012 |
| Rb-3 | $Rb_2WO_4$ | 1.070 | 1.057 | 0.500 | 0.494 |
| | | 1.378 | 1.320 | | 0.474 |
| | | 1.323 | 1.271 | | 0.478 |
| | | 1.096 | 1.076 | | 0.490 |
| Av. | | | | | 0.484 ± 0.010 |
| Rb-4 | $Rb_2WO_4$ | 2.006 | 1.944 | 0.866 | 0.839 |
| | | 1.491 | 1.504 | | 0.877 |
| | | 1.295 | 1.313 | | 0.879 |
| Av. | | | | | 0.864 ± 0.021 |

A considerable number of $Rb_xWO_3$ samples were obtained from Mr. Howard Shanks of the Ames Laboratory and analyzed for their rubidium concentrations. The x values of these bronzes varied from 0.30 to 0.43. Results of these analyses are summarized in Table 4. A comparison of Tables 3 and 4 will show that the range in x value chosen for the known mixtures more than adequately represents any variation in x value found in the bronzes.

Table 4. Thermal neutron activation analysis of the rubidium tungsten bronzes

| Sample | Samples Irradiated | Rubidium x Value |
|---|---|---|
| Rb-1A | 6 | 0.321 ± 0.013* |
| Rb-1B | 6 | 0.344 ± 0.002 |
| Rb-1C | 4 | 0.305 ± 0.009 |
| Rb-1D | 4 | 0.342 ± 0.008 |
| Rb-1E | 4 | 0.357 ± 0.021 |
| Rb-2A | 4 | 0.302 ± 0.012 |
| Rb-2B | 4 | 0.342 ± 0.012 |
| Rb-2C | 3 | 0.331 ± 0.010 |
| Rb-2D | 4 | 0.316 ± 0.002 |
| Rb-2F | 4 | 0.339 ± 0.004 |
| Rb-2G | 3 | 0.341 ± 0.002 |
| Rb-3A | 3 | 0.383 ± 0.006 |
| Rb-4 | 4 | 0.429 ± 0.003 |

*The standard deviations given represent the standard deviations of individual values of x.

## Analysis of $La_xWO_3$

The concentration of lanthanum in $La_xWO_3$ was determined nondestructively by gamma scintillation spectrometry. This technique allowed for the separation of the 1.597 Mev photopeak and the 2.09 Mev sum peak of $La^{140}$ from interfering $W^{187}$. The sum peak observed resulted from the prompt coincidence of the 2 gamma transitions (0.491 and 1.597 Mev)

associated with the decay of $La^{140}$.

Samples to be analyzed were weighed on a microbalance and encapsulated in polyethylene tubing. In all cases high purity $La_2O_3$ was used as the standard. Prior to irradiation, 4 samples of a given bronze and 3 standard samples were linearly positioned, in an alternating fashion, on Mylar tape which was then sealed over the sample. This sealed row of samples and standards was then placed in the "rabbit" for irradiation. Care was taken to insure that the package was aligned along the length of the rabbit. These precautions for packaging and alignment were necessary because the reactor thermal neutron flux was constant over the length of the rabbit, but not across its diameter. Samples and standards were then irradiated for 10 seconds in a thermal flux of $1 \times 10^{12}$ neutrons/$cm^2$ x sec.

Following bombardment, samples were counted in the well of a 4 x 4 inch Harshaw NaI(Tl) crystal which was optically coupled to an RCA 8055 photomultiplier tube. Spectral data were accumulated with the RIDL Model 24-1 multichannel analyzer. The resolution, $\eta$, of the spectrometer with this crystal was 8.8%. The read-out device used was a Friden adding machine. Each gamma-ray spectrum was graphically integrated between the limits 1.45 and 2.25 Mev by identifying the channels corresponding to these energies on paper tape and then summing the counts in the channels between these limits. This sum was divided by the accumulation live-time to convert it to activity. Activities thus determined represented only $La^{140}$ activity and were corrected for background. Samples were counted for total times of 2 minutes and generally had counting rates exceeding 10,000 cpm, thus minimizing

statistical counting errors. The activities of the standards were converted to specific activities, and lanthanum x values were calculated by using equations 8 and 9.

A self-shielding determination was made following the procedure outlined for rubidium. No self-shielding was observed for the sample and standard sizes used (5-25 and 2-5 mg).

Known mixtures of $La_2O_3$ and $WO_3$ were prepared, and mixed in a ball mill for several days. Results of the analyses of these samples are given in Table 5. Table 6 summarizes the results of the non-destructive

Table 5. Thermal neutron activation analyses of known mixtures of $La_2O_3$ and $WO_3$

| Sample | Lanthanum, mg | | x | |
|---|---|---|---|---|
| | Calculated | Observed | Calculated | Observed[a] |
| La-1A | 0.277 | 0.274 | 0.095 | 0.095 ± 0.003 |
| | 0.303 | 0.316 | | |
| | 0.267 | 0.272 | | |
| | 0.333 | 0.326 | | |
| La-1B | 0.426 | 0.400 | 0.142 | 0.137 ± 0.004 |
| | 0.535 | 0.525 | | |
| | 0.433 | 0.422 | | |
| | 0.410 | 0.411 | | |
| La-1C | 0.564 | 0.545 | 0.190 | 0.185 ± 0.004 |
| | 0.591 | 0.596 | | |
| | 0.592 | 0.597 | | |
| | 0.538 | 0.524 | | |

[a]Average of 4 determinations

neutron activation analysis of a series of $La_xWO_3$ samples which were also prepared by Mr. Howard Shanks. Good agreement between calculated and

Table 6. Thermal neutron activation analyses of the lanthanum tungsten bronzes

| Sample | Irradiations | Samples/ Irradiation | Standards/ Irradiation | x Value |
|---|---|---|---|---|
| S-1 | 1 | 4 | 3 | 0.156 ± 0.004 |
| S-2 | 1 | 4 | 3 | 0.150 ± 0.001 |
| S-3 | 3 | 4 | 3 | 0.120 ± 0.006 |
| | | 4 | 3 | 0.128 ± 0.002 |
| | | 4 | 3 | 0.121 ± 0.001 |
| S-4 | 2 | 4 | 3 | 0.119 ± 0.002 |
| | | 4 | 3 | 0.111 ± 0.003 |
| S-5 | 2 | 4/2 | 3/3 | 0.068 ± 0.001 |

experimentally observed values is seen in the case of the mixtures. No x values were reported by Mr. Shanks for the $La_xWO_3$ samples.

## Analysis of $Ho_xWO_3$

Another method of analysis whose success was largely due to scintillation spectrometry involved the nondestructive determination of holmium in $Ho_xWO_3$. For this determination, photopeaks of $Ho^{166}$ which occurred at 1.38 and near 1.6 Mev were isolated for counting from $W^{187}$ interference. That isolation of these photopeaks was accomplished was established from the analyses of mixtures with known holmium and tungsten concentrations.

Prior to irradiation, samples were weighed on a microbalance and encapsulated in polyethylene tubing. High purity $Ho_2O_3$ was in all cases used as the standard. Four samples of each bronze and 3 standard samples

were irradiated together at any one time. They were packaged and positioned inside the "rabbit" following the procedure used for the lanthanum tungsten bronzes and then irradiated for 1 to 5 seconds in a thermal flux of $1 \times 10^{13}$ neutrons/$cm^2$ x sec.

Following the irradiation, the samples were counted with a 3 x 3 inch Harshaw NaI(Tl) crystal which was optically coupled to an RCA 8054 photomultiplier tube. Spectral data were accumulated with the RIDL Model 24-1 multichannel spectrometer. The resolution, $\eta$, of the spectrometer with this crystal was 8.6%. A Friden adding machine was used as the read-out device. Each gamma-ray spectrum was graphically integrated between the limits 1.25 and 1.85 Mev following the procedure used for lanthanum. Activities thus determined represented only $Ho^{166}$ activity and were corrected for background. No decay corrections were necessary because of the long half-life of $Ho^{166}$ and the short (1-2 min.) counting times used. Counting rates usually exceeded 10,000 cpm, thus minimizing statistical counting errors. Activities of the standards were converted to specific activities, R, by dividing by the weights of holmium in the standards. Equations 8 and 9 were used to calculate the holmium x values.

Self-shielding determinations were made on samples of $Ho_2O_3$ and $Ho_xWO_3$ following the procedure outlined for rubidium in a previous section. For the sample and standard weights used, 5 to 25 and 2 to 5 mg respectively, self-shielding was not a problem.

The accuracy of the method was tested by analyzing several known mixtures of $Ho_2O_3$ and $WO_3$ which were prepared by weighing together small quantities of the oxides. For these samples, the weight ratio of holmium to tungsten approximated samples of $Ho_xWO_3$ with $0.1<x<0.2$. The results

of these analyses are summarized in Table 7. Good agreement is displayed between calculated and experimentally observed values.

Table 7. Neutron activation analysis of mixtures of $Ho_2O_3$ and $WO_3$

| Sample | W/Ho by weight | Holmium, mg | |
|---|---|---|---|
| | | Calculated | Observed |
| 1 | 10 | 0.489 | 0.492 |
| 2 | 10 | 0.441 | 0.459 |
| 3 | 10 | 0.524 | 0.518 |
| 4 | 10 | 0.415 | 0.397 |
| 5 | 5 | 0.912 | 0.916 |
| 6 | 5 | 0.803 | 0.845 |
| 7 | 5 | 0.952 | 0.970 |

Table 8 lists the results obtained for the analyses of 3 $Ho_xWO_3$ samples

Table 8. Nondestructive neutron activation analysis of holmium tungsten bronzes

| Sample | Irradiations | Samples/ Irradiation | Standards/ Irradiation | x | |
|---|---|---|---|---|---|
| | | | | Reported | Observed |
| Ho-1 | 2 | 4 | 3 | 0.100 | 0.099 ± 0.005 |
| | | | | | 0.102 ± 0.003 |
| Av. | | | | | 0.101 ± 0.004 |
| Ho-2 | 2 | 4 | 3 | 0.140 | 0.138 + 0.003 |
| | | | | | 0.144 ± 0.005 |

Table 8. (Continued)

| Sample | Irradiations | Samples/ Irradiation | Standards/ Irradiation | x Reported | x Observed |
|---|---|---|---|---|---|
| Av. | | | | | 0.141 ± 0.004 |
| Ho-3 | 2 | 4 | 3 | 0.180 | 0.172 ± 0.003 |
| | | | | | 0.174 ± 0.007 |
| Av. | | | | | 0.173 ± 0.008 |

obtained from Dr. W. Ostertag of the Wright-Patterson Air Force Base. Reported x values are based on the stoichiometric quantities of the constituents used to prepare these bronzes in a closed system by thermal reaction. Good agreement was found between these values and those experimentally obtained by activation analysis.

## Analysis of $U_xWO_3$

Gamma-rays associated with the decay of $La^{140}$ and of $I^{135}$, which are part of the uranium fission product spectrum, were utilized for the determination of uranium concentration in $U_xWO_3$. Isolation of the photopeaks of interest, in the energy range 1.45 to 2.75 Mev, from $W^{187}$ interference was accomplished by gamma scintillation spectrometry.

Samples to be analyzed were weighed on a microbalance and encapsulated in polyethylene tubing prior to irradiation. They were then packaged and positioned in the "rabbit" following the procedure used for the lanthanum tungsten bronzes. Each irradiation package consisted of 3 samples and 2 standards ($U_3O_8$), and was irradiated for 5 seconds in a

thermal flux of 1 x $10^{13}$ neutrons/$cm^2$ x sec.

Following bombardment, the samples were allowed to stand for 10 to 15 hours to allow for the decay of short-lived fission products. They were then counted for total times of 2 minutes. The spectrometer system used was identical to that used to count the holmium samples. Each gamma-ray spectrum was graphically integrated between the limits 1.45 and 2.75 Mev, and channels corresponding to these limits were identified on paper tape. Counts which occurred in the channels within these limits were then summed, and this sum was converted to activity by dividing by the accumulation live-time. Activities thus determined represented only $La^{140}$ activity, with some small contribution from $I^{135}$, and were corrected for background. Statistical counting errors did not exceed 1.5% because of the sample counting rates which were generally 5,000-10,000 cpm. Activities of the standards were converted to specific activities, and sample x values were calculated with equations 8 and 9.

In order to determine the accuracy of the analytical method, several known mixtures were prepared by weighing together finely ground $U_3O_8$ and $WO_3$ and allowing them to rotate in a ball mill for several days. Results of the analyses of these mixtures are given in Table 9. Excellent agreement between calculated and experimentally obtained values is observed for these samples, the greatest discrepancy occurring in the analysis of sample U-2A. These results indicate that uranium may be accurately determined in the presence of tungsten by the procedures described.

Results of the analyses of several $U_xWO_3$ samples are summarized in Table 10. The reported x values are based on the stoichiometric quantities

Table 9. Thermal neutron activation analyses of known mixtures of $U_3O_8$ and $WO_3$

| Sample | Samples Irradiated | Standards Irradiated | Uranium, Mg | | x | |
|---|---|---|---|---|---|---|
| | | | Calculated | Observed | Calculated | Observed[a] |
| U-1A | 4 | 3 | 0.441 | 0.448 | 0.060 | 0.060 ± 0.001 |
| | | | 0.403 | 0.421 | | |
| | | | 0.313 | 0.317 | | |
| | | | 0.339 | 0.335 | | |
| U-2A | 4 | 3 | 0.621 | 0.561 | 0.080 | 0.086 ± 0.003 |
| | | | 0.598 | 0.553 | | |
| | | | 0.481 | 0.469 | | |
| | | | 0.523 | 0.469 | | |
| U-3A | 4 | 3 | 0.565 | 0.583 | 0.100 | 0.100 ± 0.003 |
| | | | 0.599 | 0.614 | | |
| | | | 0.516 | 0.517 | | |
| | | | 0.635 | 0.619 | | |
| U-4A | 4 | 3 | 0.783 | 0.795 | 0.120 | 0.121 ± 0.001 |
| | | | 0.397 | 0.403 | | |
| | | | 0.545 | 0.544 | | |
| | | | 0.561 | 0.567 | | |

[a]Average of 4 determinations

Table 10. Thermal neutron activation analysis of the uranium tungsten bronzes

| Sample | Samples Irradiated | Standards Irradiated | x | |
|---|---|---|---|---|
| | | | Reported | Observed |
| U-1 | 6 | 4 | 0.078 | 0.077 ± 0.002 |
| U-2 | 6 | 4 | 0.080 | 0.080 ± 0.001 |
| U-3 | 6 | 4 | 0.083 | 0.087 ± 0.002 |
| U-4 | 6 | 4 | 0.090 | 0.096 ± 0.002 |
| U-5 | 6 | 4 | 0.100 | 0.100 ± 0.002 |

of the constituents used to prepare these samples in a closed system by thermal reaction. These samples were also supplied by Dr. Ostertag.

## ACTIVATION WITH 14 Mev NEUTRONS

### Introduction

Attempts were made to analyze for barium in $Ba_xWO_3$ by thermal neutron activation, but the barium activities, particularly 83m. $Ba^{137m}$, were not produced in sufficient intensity compared to the 24 hour $W^{187}$ to permit quantitative determination. For this reason an activation scheme was developed using 14 Mev neutrons. The reactions produced in $Ba_xWO_3$ by 14 Mev neutrons are listed in Table 11. (52,53) Figures 12 and 13 represent

Table 11. Products of short term irradiation of $Ba_xWO_3$ with 14 Mev neutrons

| Radioactive Product | Product Half-life | Precursor | Isotopic Abundance (%) | Reaction | Principal Gamma-rays (Mev) |
|---|---|---|---|---|---|
| $Ba^{137m}$ | 2.6m | $Ba^{136}$ | 7.81 | n,γ | 0.662 |
| | | $Ba^{137}$ | 11.32 | n,n' | |
| | | $Ba^{138}$ | 71.66 | n,2n | |
| $W^{185m}$ | 1.7m | $W^{184}$ | 30.64 | n,γ | 0.125, 0.175 |
| | | $W^{186}$ | 28.41 | n,2n | |
| $N^{16}$ | 7.35s | $O^{16}$ | 99.76 | n,p | 6.13, 7.12 |

the gamma-ray scintillation spectra of $Ba^{137m}$ and of a $Ba_xWO_3$ sample with x = 0.054 respectively. These spectra were accumulated 30 seconds after irradiation to allow for the decay of $N^{16}$ produced by the reaction $O^{16}(\gamma,p)N^{16}$. It can be seen that the $Ba^{137m}$ photopeak is well resolved from any interferences.

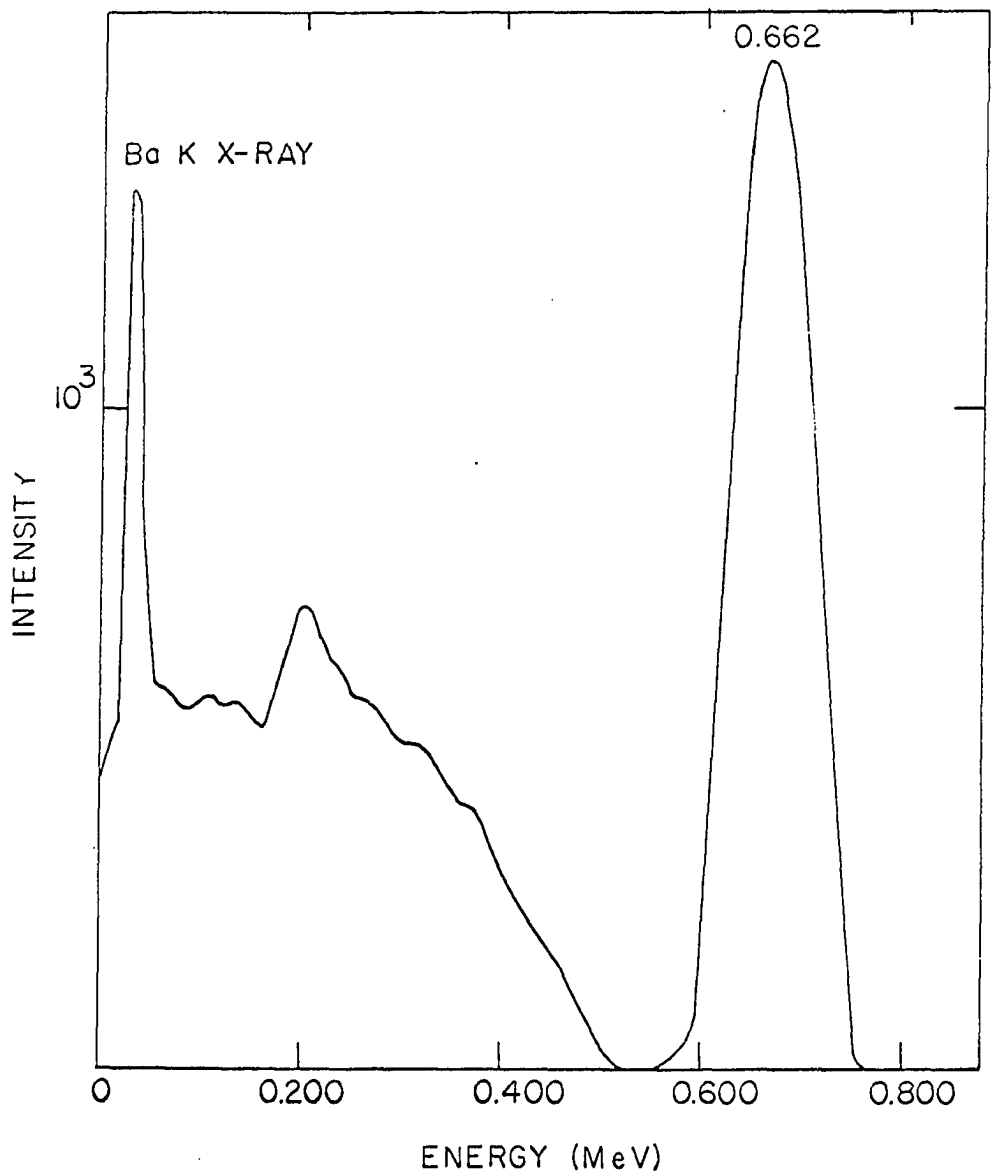


Figure 12. Gamma-ray spectrum of $Ba^{137m}$

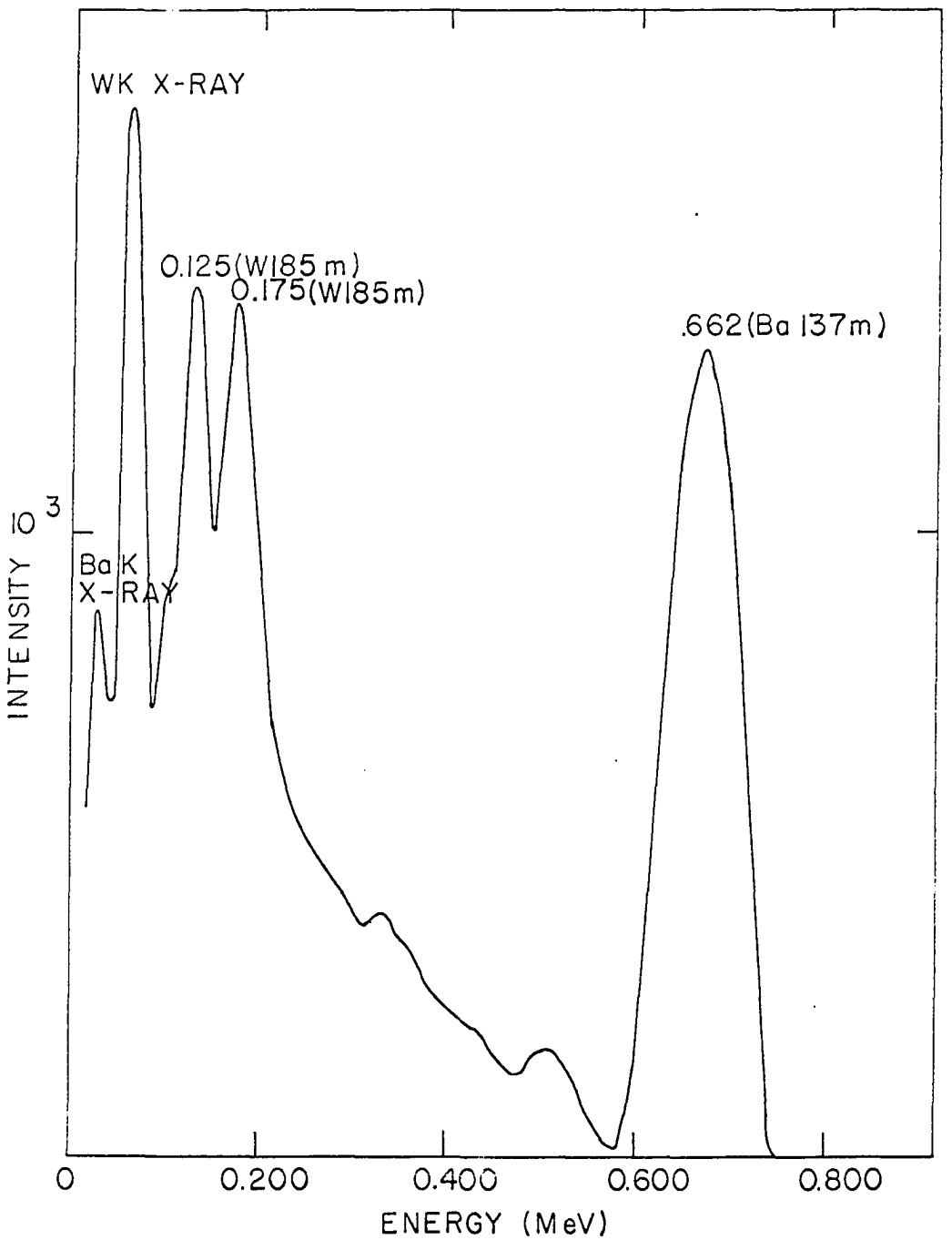


Figure 13. Gamma-ray spectrum of $Ba_{0.05}WO_3$ following irradiation with 14 Mev neutrons

## Neutron Source

Samples were irradiated in the fast neutron flux of a Texas Nuclear Corporation Model 9900 neutron generator. This is a Cockroft-Walton type accelerator, producing 15 kev deuterons, with a maximum current of 2.5 ma. A $4\pi$ yield of $2.5 \times 10^{11}$ 14 Mev neutrons per second can be produced by the reaction $T(d,n)He^4$ if the deuterons impinge on a new, 3-5 curie/$in^2$ tritiated titanium target.

Samples were transferred to and from the irradiation site in a modified TNC pneumatic transfer system, Model 9610. The irradiation and counting equipment were automatically programmed for operation with a TNC Model 9615 programmer. The system was modified for use by Messrs. Richard Clark and Wayne Stensland of the Ames Laboratory Radiochemistry Group I.

## Analysis of $Ba_xWO_3$

Samples to be analyzed were finely powdered with agate mortar and pestle and weighed into polyethylene ampoules, which were in turn placed in paraffin capsules, cylindrical in shape and having the dimensions 1 1/4 x 1/2 inch. The holes which were drilled in the cylinders to accommodate the samples were 1 1/8 x 1/4 inch. Because of the variation in the fast neutron flux, it was necessary to irradiate a suitable combination flux monitor and standard along with each sample. Finely powdered $BaCO_3$ was used for this purpose. A weighed amount was distributed evenly around the polyethylene ampoule so as to completely surround it. The irradiation cylinder was then carefully sealed with hot, liquid paraffin and placed in a polyethylene "rabbit" for transfer to the target. Figure 14 depicts the irradiation cylinder and polyethylene

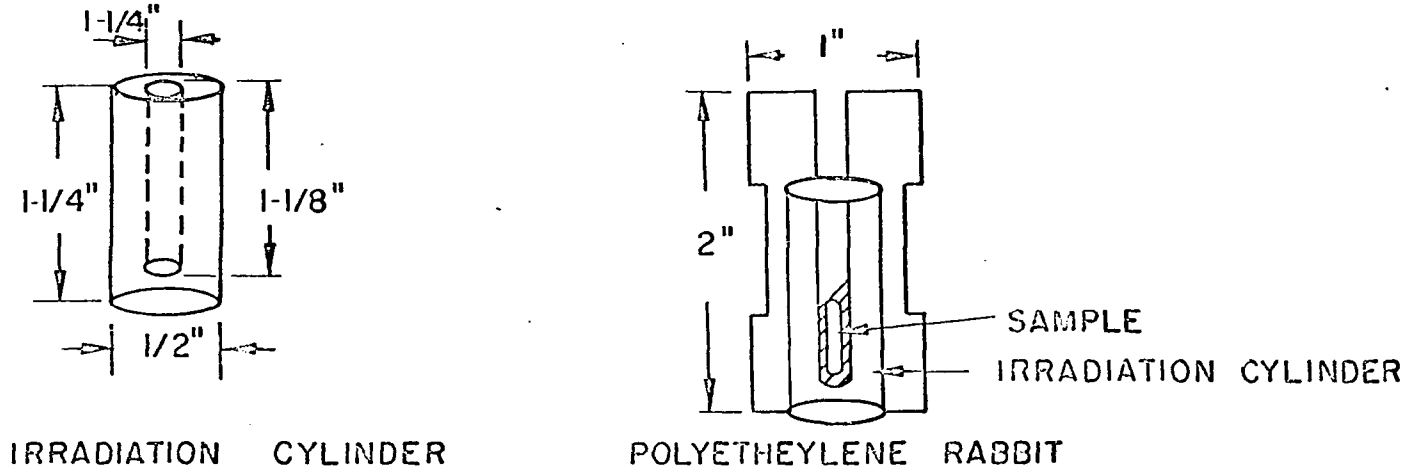


Figure 14. Irradiation cylinder and polyethylene rabbit

rabbit used in this work.

During the one minute irradiation period the sample was mechanically rotated, at about 300 rpm, at a distance of approximately one inch from the target. Following irradiation the sample was pneumatically transferred back to the counting laboratory with a transit time of one second. Nitrogen was used to transfer the sample. The paraffin cylinder was mechanically separated from the polyethylene "rabbit" and allowed to drop into the well of a 4 x 4 inch Quartz Products NaI(Tl) crystal. A removable iron thimble was suspended in the well to protect the crystal.

The 4 x 4 inch NaI(Tl) crystal was optically coupled to an RCA 8055 photomultiplier tube. The output from this detector was fed to an RIDL Model 34-12 B gamma-ray scintillation spectrometer which was used, in connection with a scaler, for the activity measurements. In this case, the multichannel analyzer was programmed to act as a single channel analyzer, with read-out on the scaler.

For this analysis the activity of interest was 2.6 minute $Ba^{137m}$ which decays by an isomeric transition with a 662 kev gamma-ray. This is the "$Cs^{137}$" gamma-ray commonly used for calibration of gamma-ray spectrometers. The photoelectric peak from this gamma-ray was counted. The only interfering activity was from Compton scattering of the high energy gamma-rays of $N^{16}$. This was eliminated by allowing the sample to decay for 30 seconds before counting. After this delay the paraffin cylinder which contained both the sample and standard was counted for 60 seconds. The paraffin cylinder was then broken and discarded along with the standard material, leaving the sample ampoule to be counted for another 60 seconds. One minute was allowed for the separation. The

second, or sample count, was corrected for its decay and subtracted from the total activity in order to find the activity due to the standard. Since the weight of barium in the standard was known, its specific activity could be calculated and used to determine the percent of barium present in the sample. Barium x values were calculated by using equation 9.

Preliminary work done in developing an analytical method for barium involved the irradiation of pure $BaCO_3$ in both the sample and standard/flux monitor positions. The results obtained are summarized in Table 12.

Table 12. Analysis of $BaCO_3$ by fast neutron activation analysis

| Sample | No. of Irradiations | Milligrams of Barium in Sample | |
|---|---|---|---|
| | | Calculated | Observed[a] |
| 1 | 2 | 10.70 | 10.96 |
| 2 | 2 | 9.83 | 9.85 |
| 3 | 2 | 9.56 | 9.73 |

[a]Average of two irradiations

Barium x values were determined for an artificial barium-tungsten mixture with a known x value which was made by mixing together weighed amounts of $BaCO_3$ and $WO_3$, and for a $Ba_xWO_3$ sample. Table 13 summarizes the results obtained for these analyses. It can be seen that the experimentally obtained values show good agreement with those calculated in the case of the mixture and, within the limit of error, with the chemical analysis of $Ba_xWO_3$. The $Ba_xWO_3$ sample was obtained from Dr. L. Conroy of the University of Minnesota.

Table 13. Fast neutron analysis of a Ba-W mixture (A-1) and a barium tungsten bronze (B-C-1)

| Sample | No. of Irradiations | Mg. of Ba | | x |
|---|---|---|---|---|
| | | Calculated | Observed | |
| A-1 | 2 | 9.95 | 10.05 | 0.120 ± 0.001 |
| | 2 | 9.67 | 9.22 | 0.114 ± 0.004 |
| | 2 | 10.17 | 10.08 | 0.118 ± 0.003 |
| | Av. | | | 0.117 ± 0.003 |
| | Theoretical | | | 0.119 |
| B-C-1 | 2 | | 4.76 ± 0.19 | 0.054 ± 0.001 |
| | 3 | | 4.74 ± 0.05 | 0.054 ± 0.001 |
| | 3 | | 4.12 ± 0.11 | 0.056 ± 0.001 |
| | Av. | | | 0.054 ± 0.001 |
| | Chemical Analysis (2) | | | 0.061 ± 0.005 |

# HIGH ENERGY PHOTON ACTIVATION

## Introduction

The nuclear reactions involved in the irradiation of the tungsten bronzes of potassium, gadolinium and europium with high energy photons are summarized in Table 14. The fact that it was not possible to assure flux homogeneity in the simultaneous irradiation of more than one sample precluded the use of comparator standards. Thus, the combined spectrum of $Ta^{184}$ and $Ta^{185}$ was used as an internal standard for the analyses of $Gd_xWO_3$ and $Eu_xWO_3$. In the case of the potassium tungsten bronzes, the activity in the 2.16 Mev photopeak of $K^{38}$ was compared to that in the combined 0.060, 0.075 Mev photopeak of $Ta^{185}$.

Figures 15 and 16 represent gamma-ray scintillation spectra of the tantalum isotopes. Gamma-ray spectra of $K_2CO_3$, $K_{0.4}WO_3$, $Gd_2O_3$, $Gd_{0.15}WO_3$, $Eu_2O_3$ and $Eu_{0.15}WO_3$ are given in Figures 17-22. From a consideration of Figures 19-22, it is apparent that no simple internal standard technique could be used for the analyses of $Gd_xWO_3$ and $Eu_xWO_3$. The rare-earth and tantalum photopeaks were not sufficiently resolved from one another to allow for this type of comparison.

## Irradiation Source

Irradiations were made by using the bremsstrahlung from the Iowa State University electron synchrotron. Irradiations were made for time periods of 5 to 20 minutes. Samples to be analyzed were positioned by means of a probe arrangement inside the acceleration chamber of the synchrotron operating at 70 Mev. The 70 Mev electrons impinge on a lead target to produce bremsstrahlung, electromagnetic radiation of all energies

Table 14. Nuclear properties of the constituents of $K_xWO_3$, $Gd_xWO_3$ and $Eu_xWO_3$ subjected to irradiation with high energy photons

| Target Nuclide | Abundance (%) | Reaction | Reaction Product | Product Half-life | Principal Gamma-rays (Mev) |
|---|---|---|---|---|---|
| $W^{186}$ | 28.41 | γ,n | $Ta^{185}$ | 49m | 0.060, 0.075, 0.100, 0.175, 0.245 |
| | | γ,pn | $Ta^{184}$ | 8.7h | 0.408, 0.413 |
| $K^{39}$ | 93.10 | γ,n | $K^{38}$ | 7.7m | 0.511 ($\beta^+$), 2.16 |
| $Gd^{160}$ | 21.90 | γ,n | $Gd^{159}$ | 18h | 0.058, 0.364 |
| $Eu^{153}$ | 52.18 | γ,n | $Eu^{152}$ | 9.3h | 0.122, 0.344, 0.511 ($\beta^+$) 0.842, 0.963 |
| $O^{16}$ | 99.759 | γ,n | $O^{15}$ | 124s | 0.511 ($\beta^+$) |
| | | γ,p2n | $N^{13}$ | 9.96m | 0.511 ($\beta^+$) |
| | | (γ,dn) | | | |

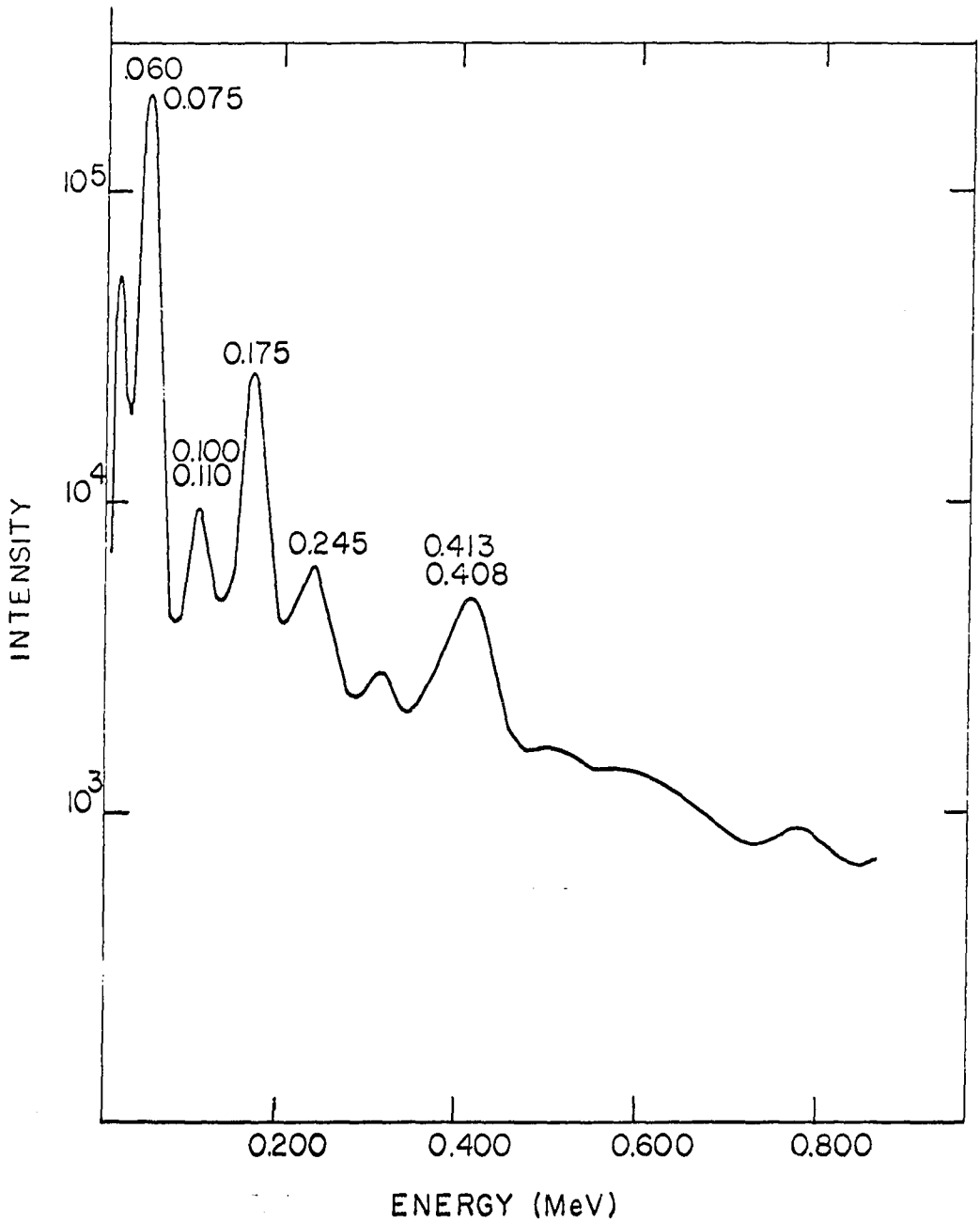


Figure 15. Gamma ray spectrum of $Ta^{184}$ and $Ta^{185}$

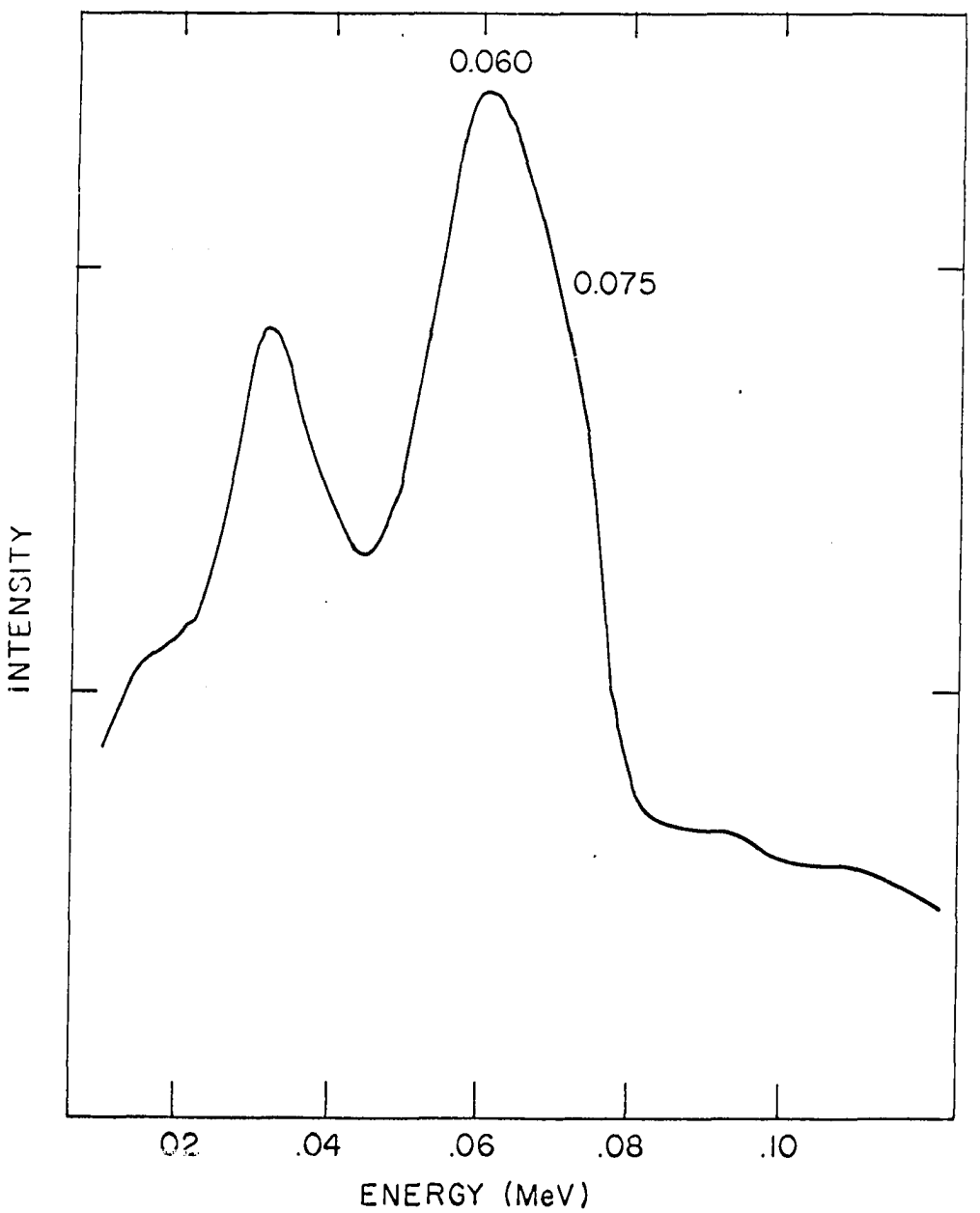


Figure 16. Gamma-ray spectrum of low energy $Ta^{185}$ photopeaks

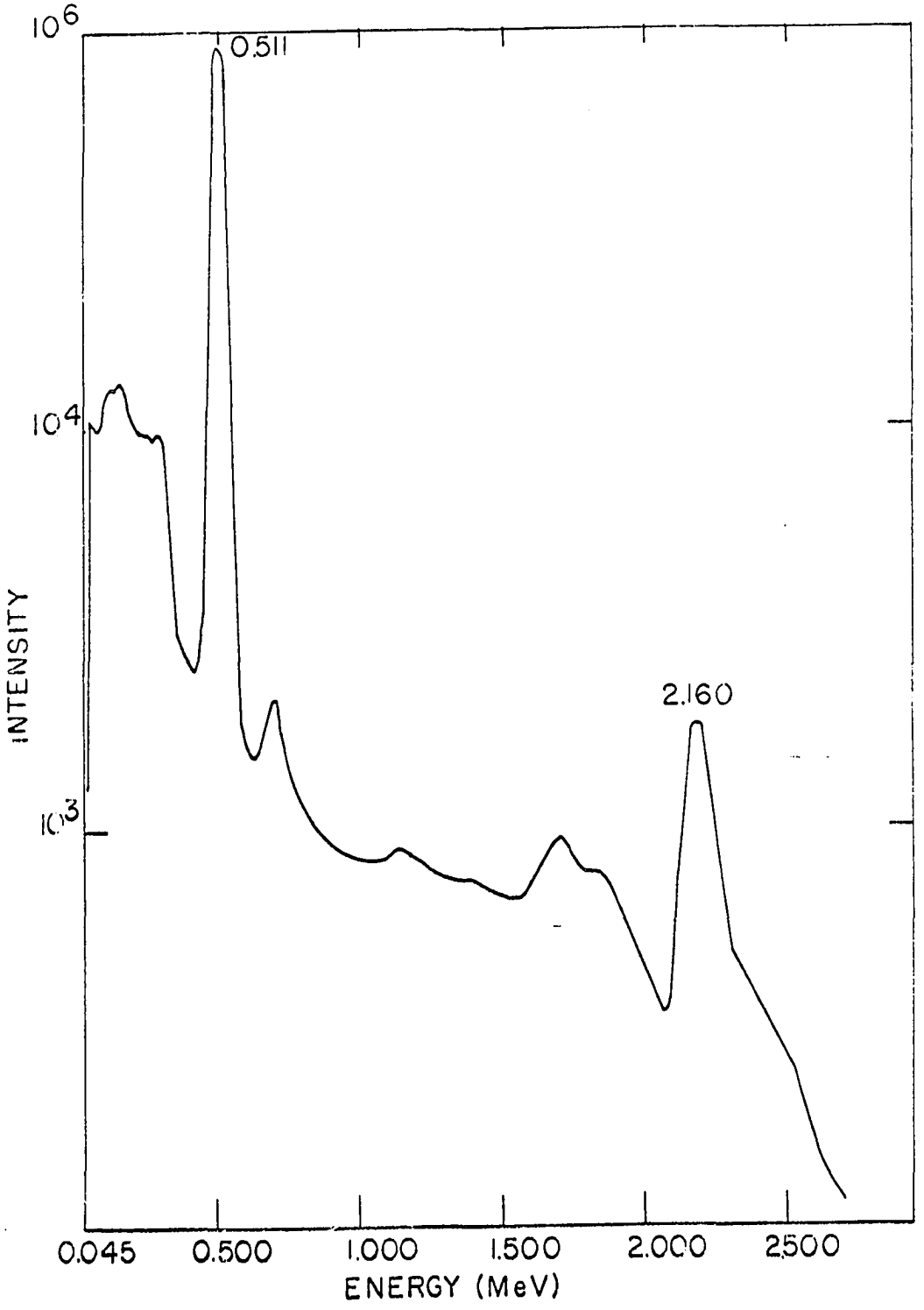


Figure 17. Gamma-ray spectrum of $K_2CO_3$ following bombardment with high energy photons

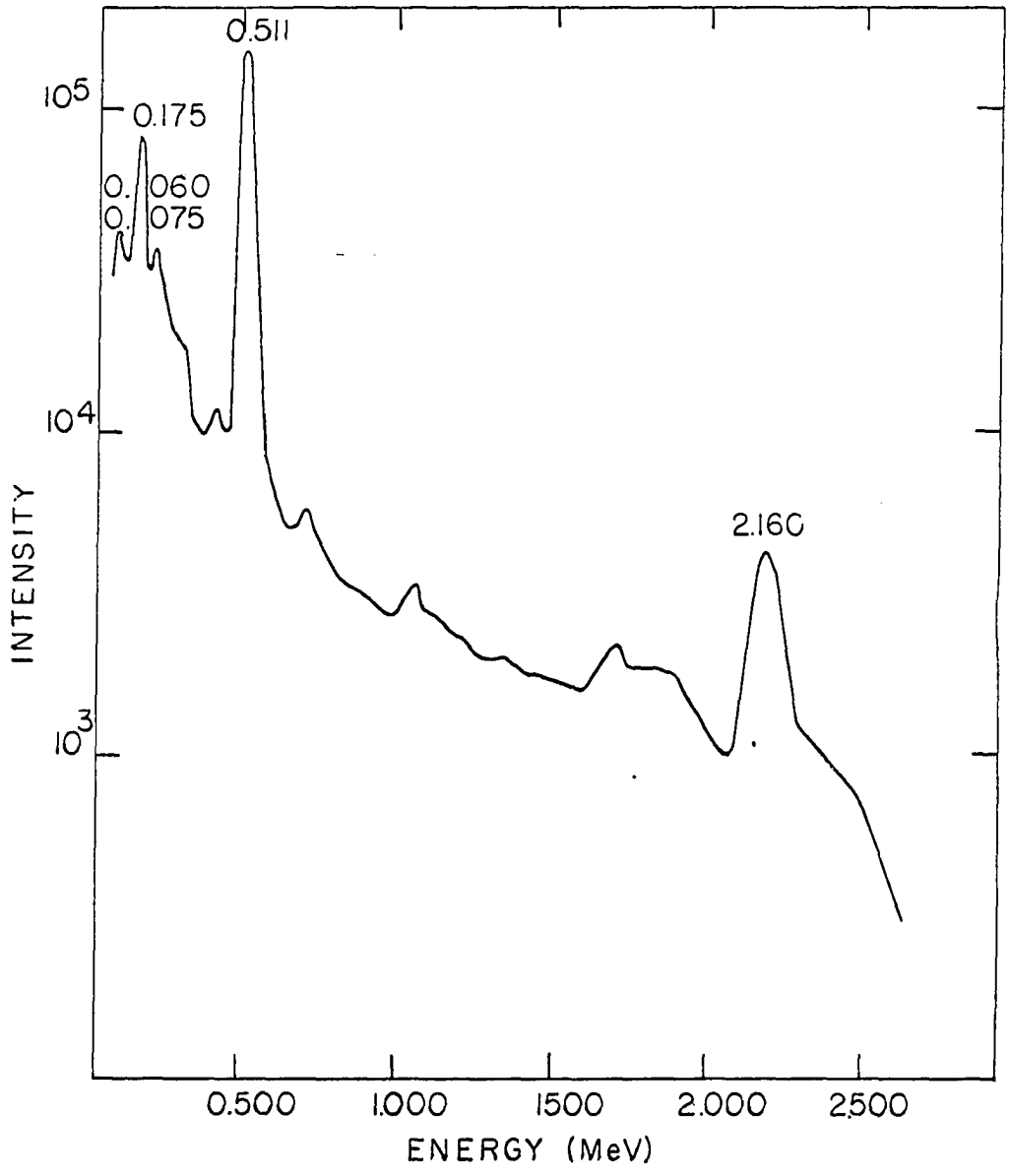


Figure 18. Gamma-ray spectrum of $K_{0.4}WO_3$ following bombardment with high energy photons

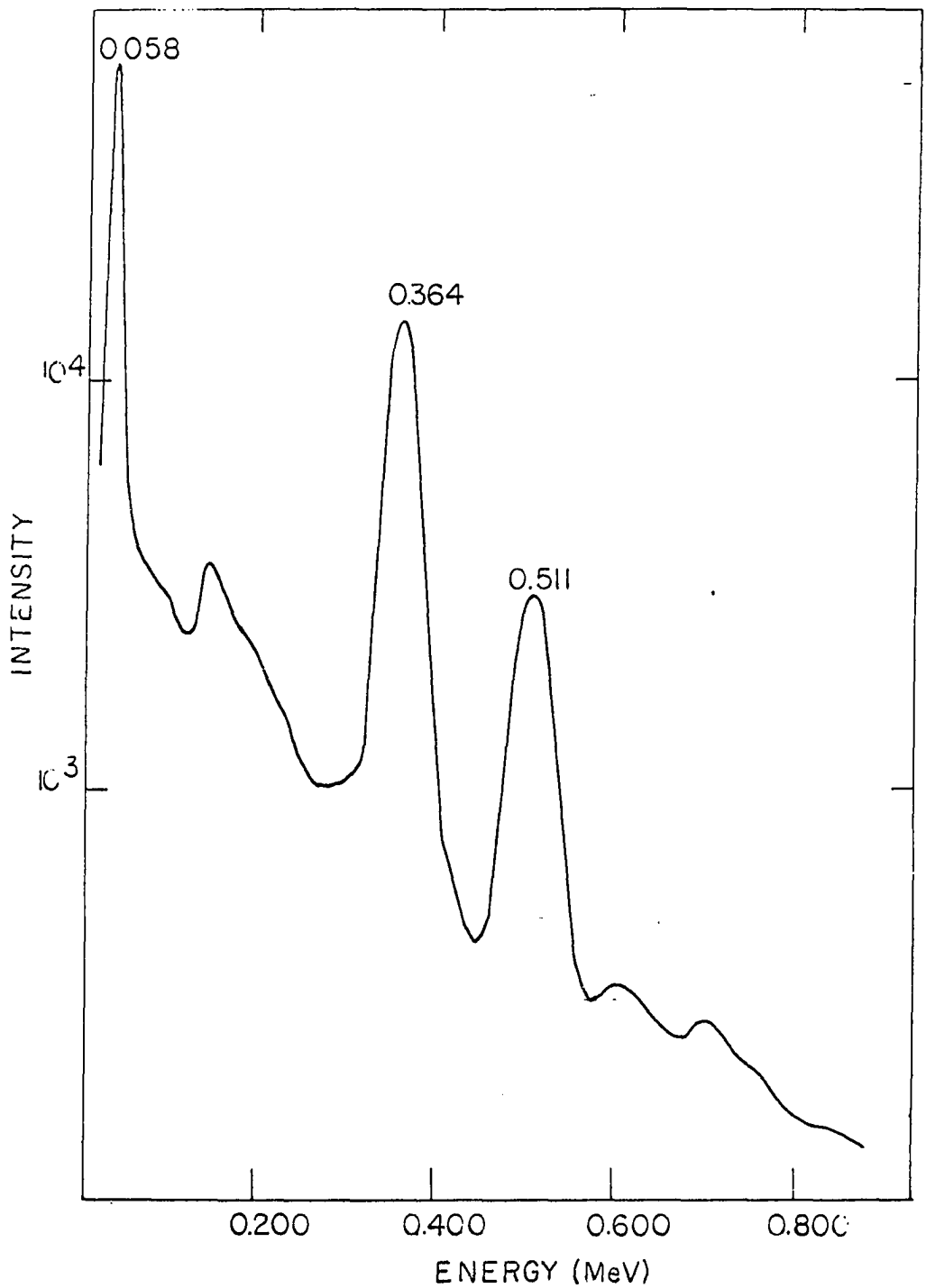


Figure 19. Gamma-ray spectrum of $Gd_2O_3$ following bombardment with high energy photons

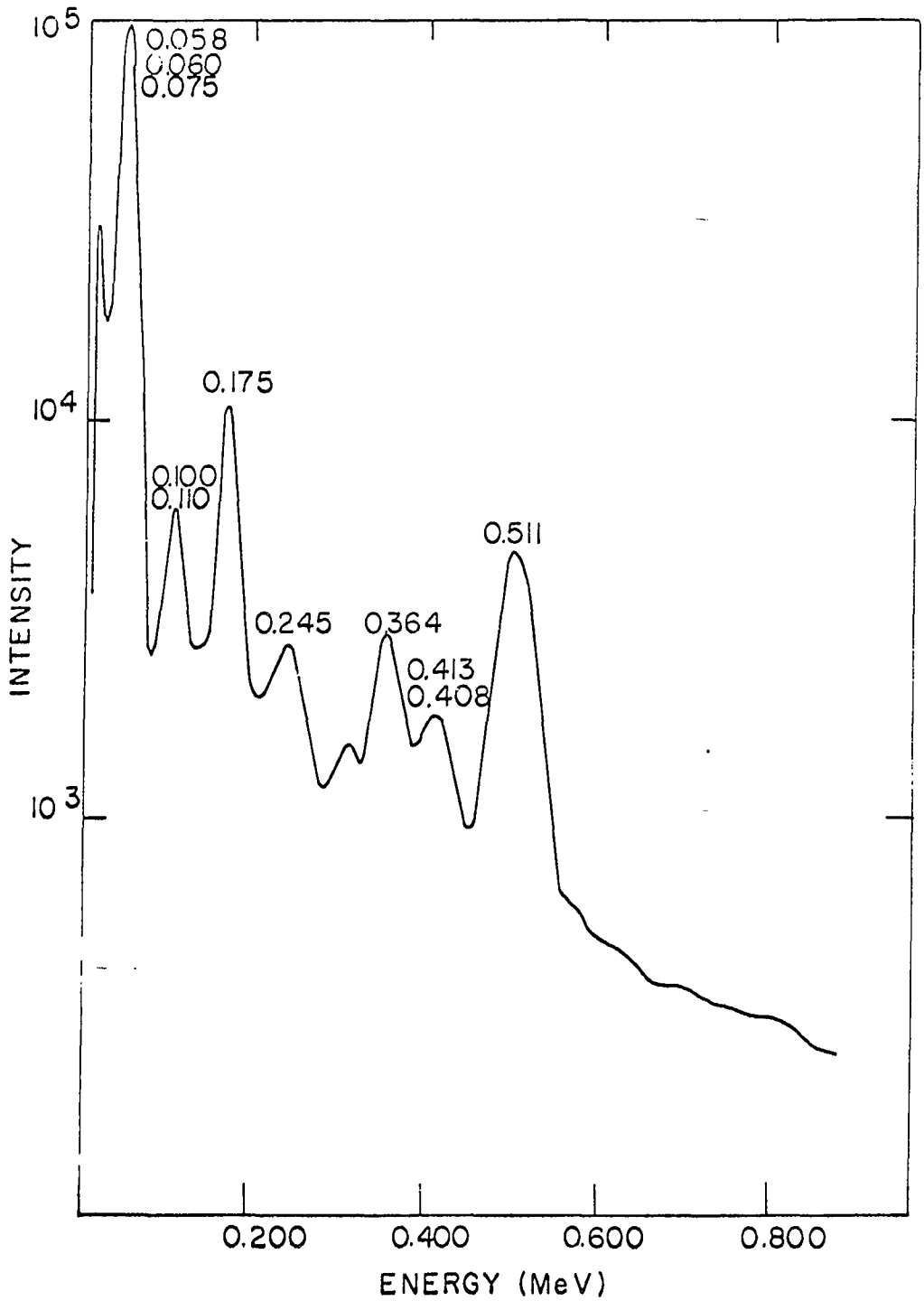


Figure 20. Gamma-ray spectrum of $Gd_{0.15}WO_3$ following bombardment with high energy photons

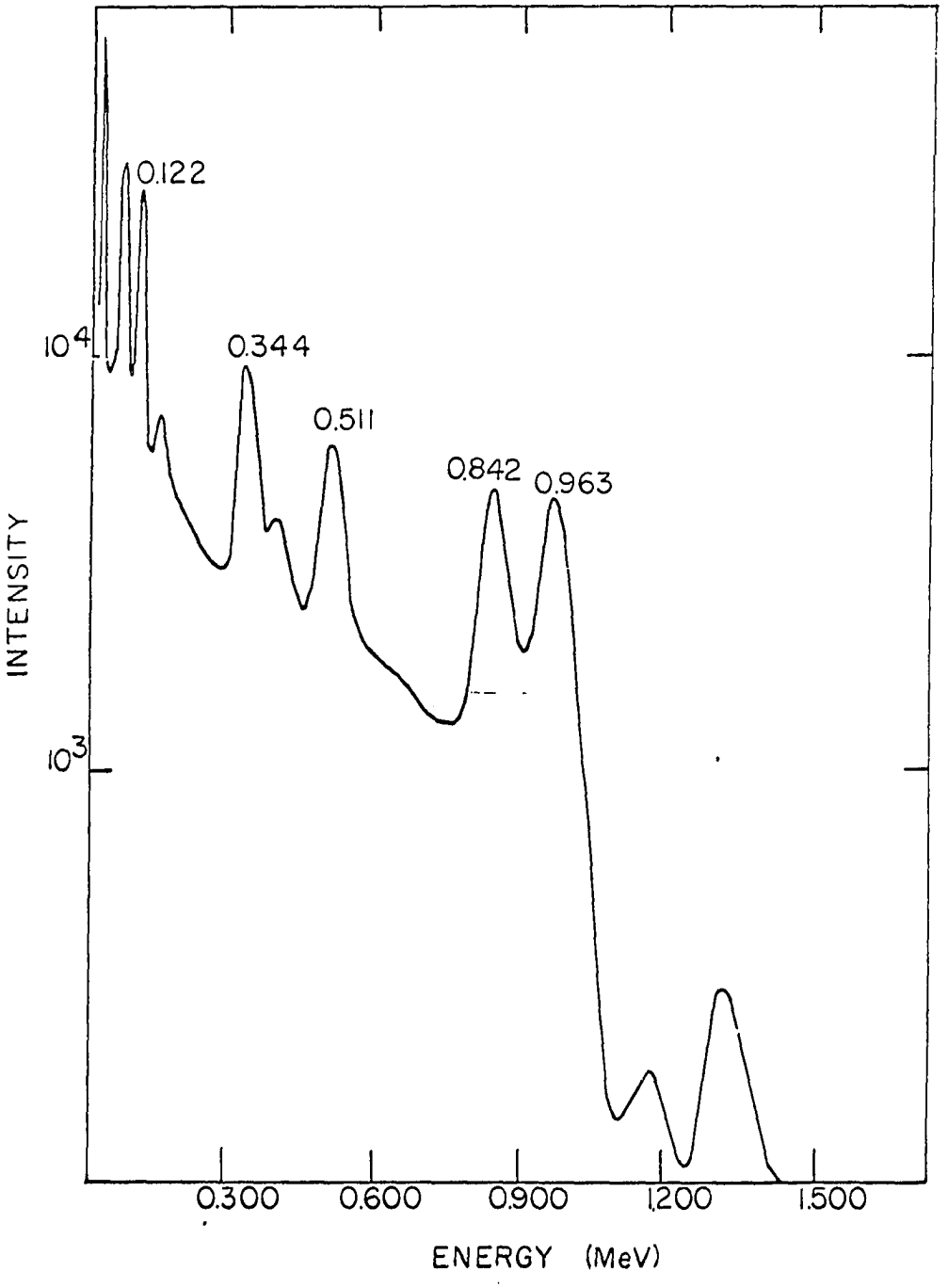


Figure 21. Gamma-ray spectrum of $Eu_2O_3$ following bombardment with high energy photons

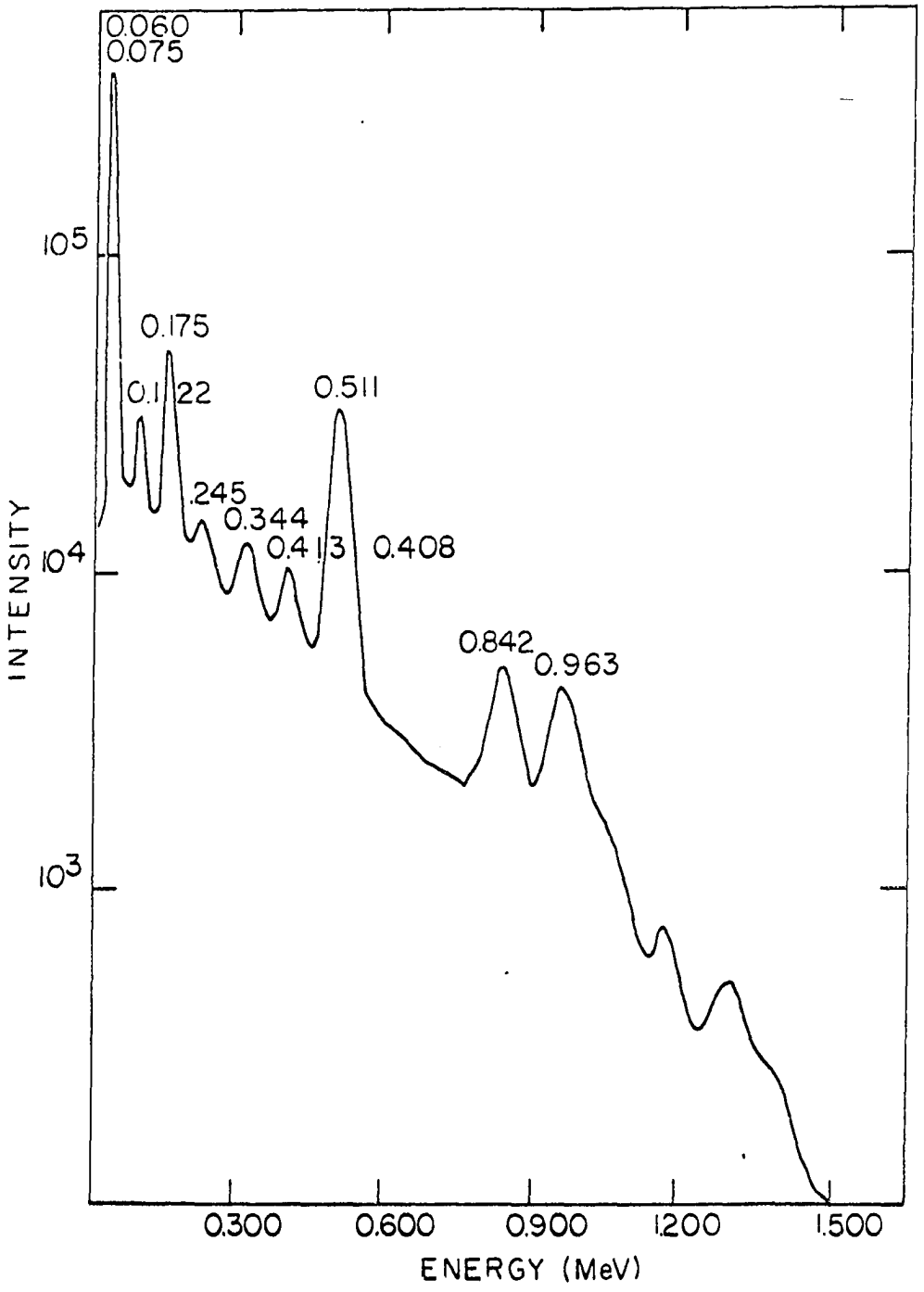


Figure 22. Gamma-ray spectrum of $Eu_{0.15}WO_3$ following bombardment with high energy photons

up to 70 Mev, which passes through the samples. The conditions of the irradiation with this accelerator have been discussed in detail by Hammer and Bureau. (54) Aluminum cans were fabricated to contain the samples during irradiation.

## Analysis of $K_xWO_3$

The internal standard technique was used to determine potassium in $K_xWO_3$. Potassium-39 when irradiated in the bremsstrahlung beam of the synchrotron undergoes the $(\gamma,n)$ reaction to produce 7.7 minute $K^{38}$, while 49 minute $Ta^{185}$ is produced by the $(\gamma,p)$ reaction on $W^{186}$. These two activities were compared using the photoelectric peak from the 2.16 Mev gamma-ray of $K^{38}$, and for $Ta^{185}$ a low energy peak which was a composite of a 60 kev x-ray and a 75 kev gamma-ray, with some contribution from Compton scattering of higher energy gamma-rays.

Decay curves for both the $K^{38}$ and $Ta^{185}$ activities were analyzed. It was found that the half-life of the 2.16 Mev gamma-ray was 7.7 minutes, which corresponded with the literature value. (50) However, the low energy composite peak, while it was primarily due to the decay of $Ta^{185}$, also included several other activities. Because of the half-lives of these activities and the contributions which they made to the total activity, it was not possible to accurately resolve the decay curves. It was, however, possible to use this composite peak as the standard activity by counting it at identical times after irradiation.

All synchrotron bombardments were 10 minutes in duration. Following an irradiation, the active sample was divided into 3 portions and placed in separate counting vials to provide counting data in triplicate. Samples were counted on a 3 x 3 inch Harshaw NaI(Tl) crystal which was

optically coupled to an RCA 8054 photomultiplier tube. An RIDL Model 24-1 multichannel gamma-ray spectrometer with read-out on a Friden adding machine was used for the activity measurements. Counts occurring in the regions of interest were graphically integrated between limits chosen by inspection of the paper tape, and summed.

The $K^{38}$ was determined first by measuring the 2.16 Mev gamma-ray peak. For comparison these activities were corrected for decay to the end of the irradiation. At approximately 55 minutes after irradiation, the activity of tungsten present was determined by measuring the low energy composite peak. These activities were corrected to t = 55 minutes by means of a working curve which was constructed for this purpose. All activities were corrected for background. A ratio was thus obtained which related the $K^{38}$ activities at t = 0 to the tungsten activity at t = 55 minutes. The ratios obtained for the $K_xWO_3$ samples were compared to the ratio obtained for $K_2WO_4$. Because $K_2WO_4$ is a stoichiometric compound with a K/W ratio of 2.00, it was possible to determine the potassium x values for the tungsten bronzes by the equation

$$x = 2\,\frac{A^{1}K(t = 0)/A^{1}W(t = 55m)}{A^{11}K(t = 0)/A^{11}W(t = 55m)}\,, \qquad (10)$$

where the A's represent activities and the superscripts 1 and 11 indicate the tungsten bronze and the standard $K_2WO_4$ respectively.

The accuracy of the method was assured by analyzing 3 known mixtures which were prepared by mixing together weighed quantities of $WO_3$ and $K_2WO_4$ such that the ratio K/W was known. These mixtures were rotated in a ball mill for several days to assure homogeneity. Three or four samples of each mixture were irradiated, divided into 3 portions, and counted. The

$Ta^{185}$ activity induced in the samples was in all cases no greater than that in the standard. Because less material was available the weights of these samples were in general less than those of the standards. This also served to reduce the $Ta^{185}$ activity in the samples. For the standard $K_2WO_4$, 6 irradiations were made, giving a total of 18 samples for analysis. The measured ratio of activities of potassium (at t = 0) to tungsten (at t = 55m) was 2.66 ± 0.03. Table 15 summarizes the results obtained for the analyses of the known mixtures.

Table 15. Analysis for potassium in $K_2WO_4$ - $WO_3$ mixtures

| Sample | Irradiations | Samples/ Irradiation | x | |
|---|---|---|---|---|
| | | | Calculated | Observed |
| K-4 | 4 | 3 | 0.400 | 0.411 ± 0.013 |
| K-5 | 3 | 3 | 0.500 | 0.506 ± 0.006 |
| K-6 | 3 | 3 | 0.600 | 0.606 ± 0.014 |

This method has also been applied to a large number of actual potassium tungsten bronzes supplied by Mr. H. Shanks of the Ames Laboratory. The results obtained for some of these analyses are given in Table 16.

Table 16. Analysis for potassium in $K_xWO_3$

| Sample | Irradiation | Samples/Irradiation | Potassium x value |
|---|---|---|---|
| K-8E | 3 | 3 | 0.572 ± 0.012 |
| K-8B | 3 | 3 | 0.542 ± 0.010 |

Table 16. (Continued)

| Sample | Irradiation | Samples/Irradiation | Potassium x value |
|---|---|---|---|
| K-8L | 3 | 3 | 0.515 ± 0.013 |
| K-8I | 3 | 3 | 0.498 ± 0.003 |
| K-8J | 3 | 3 | 0.471 ± 0.007 |
| K-8R | 3 | 3 | 0.416 ± 0.009 |
| K-10C | 3 | 3 | 0.365 ± 0.006 |
| K-8V | 3 | 3 | 0.329 ± 0.008 |
| K-2B | 3 | 3 | 0.298 ± 0.005 |
| K-2D | 3 | 3 | 0.276 ± 0.003 |

## Analysis of $Gd_xWO_3$ and $Eu_xWO_3$

The bronzes of gadolinium and europium were unsuited to activation with thermal neutrons because of the extremely large activation cross sections of some of their stable isotopes. Similarly, unfavorable cross section and half-life characteristics precluded their quantitative determination by fast neutron activation.

A suitable method for the quantitative determination of these rare earths in their tungsten bronzes was devised. This method used the synchrotron as the irradiation source, and relied on a computer program for data analysis.[3] The program was written in Fortran IV for use with

[3]Korthoven, P. J. M., Ames, Iowa. Use of a computer program to resolve a gamma-ray spectrum into its components. Private communication. 1967.

the IBM 360-50 computer.

The analysis was performed using a linear least squares fitting program. This program requires information about all components present in the spectrum after irradiation. A component need not be a single isotope, but may be a mixture of several, so long as sample and standard are counted at exactly the same time after irradiation and identical irradiation times are used. The sample spectrum is assumed to be a linear combination of the component spectra. The program allows coarse and fine gain adjustments to be made, the latter by an iterative procedure to which a direct search method is applied.

In the case of the gadolinium tungsten bronzes $Gd_2O_3$ and tungsten metal were irradiated, in the manner described for $K_xWO_3$, for periods of 5 and 20 minutes. These standards were counted on a Harshaw 3 x 3 inch NaI(Tl) ($Am^{241}$) crystal which was optically coupled to an RCA 8054 photomultiplier tube. Spectra were accumulated with an RIDL Model 34-12 B gamma scintillation spectrometer. Gain shifts were minimized with an RIDL Model 39-6 gain stabilizer.

Standard spectra were accumulated at predetermined times following irradiation, with accumulation live-times of 5 or 20 minutes. Read out was accomplished with a Tally punch. Data accumulated in this manner was transferred to IBM cards for computer processing by means of a tape to card converter.

The $Gd_xWO_3$ samples were irradiated and counted following the same procedures and using exactly the same times as for the standard spectra. Using the standard spectra as references, the computer program was able to resolve each $Gd_xWO_3$ spectrum into its individual components. Contri-

bution from annihilation radiation associated with positron emission from the decay of $N^{13}$ was accounted for in the spectrum by including a positron spectrum in the standard library.

Results obtained after data processing were in the form of relative activities of gadolinium and tungsten. For each series of irradiations, at least one known mixture of gadolinium and tungsten was also irradiated. This mixture had the ratio Gd/W = 0.2 and served as a standard sample. Gadolinium x values were then calculated by comparing the relative activities obtained to those obtained for this standard sample.

The accuracy of the method was assured by analyzing a series of known mixtures having $0.005<x<0.10$, which were made by weighing together quantities of $Gd_2O_3$ and $WO_3$ and allowing them to rotate in a ball mill for several days. The results of these analyses are given in Table 17. It should be noted that different irradiation and counting times were sometimes used. This was necessitated by the fact that for samples of low x value measurements were only accurate for gadolinium after all positron activity had decayed away. Prior to this time there appeared to be competition in the program between the $Gd^{159}$ photopeak and the more intense $\beta^+$ annihilation peak, which led to discrepancies in the results.

Table 18 summarizes the results obtained for a series of bronze samples. The reported x values were based on the stoichiometric quantities of the constituents used to prepare these samples by thermal reaction. On the basis of the results obtained for the known mixtures as compared to the calculated x values, it would appear that some of the reported x values in Table 18 are in error. In both cases, the known mixture of Gd/W = 0.2 was used as the comparator standard.

Table 17. Analysis for Gd in $Gd_2O_3$ - $WO_3$ mixtures

| Sample | Irradiation Time (min) | Time of First Count After Irradiation (min) | Accumulation Time (min) | Number of Spectra Accumulated | x value | |
|---|---|---|---|---|---|---|
| | | | | | Calculated | Observed |
| 1 | 5 | 58 | 5 | 4 | 0.100 | 0.100 ± 0.001 |
| 2 | 20 | 240 | 5 | 3 | 0.050 | 0.050 ± 0.001 |
| 3 | 20 | 240 | 5 | 3 | 0.030 | 0.028 ± 0.001 |
| 4 | 20 | 240 | 5 | 3 | 0.010 | 0.0097 ± 0.0004 |
| | 20 | 1370 | 20 | 1 | 0.010 | 0.0107 ± 0.0005[a] |
| 5 | 20 | 1370 | 20 | 1 | 0.005 | 0.0051 ± 0.0003[a] |

[a]Standard deviation in relative activities

Table 18. Analysis for Gd in $Gd_xWO_3$

| Sample | Irradiation Time (min) | Time of First Count After Irradiation (min) | Accumulation Time (min) | Number of Spectra Accumulated | x value Reported | x value Observed |
|---|---|---|---|---|---|---|
| A | 20 | 240 | 5 | 3 | 0.15 | 0.1510 ± 0.0017 |
| B | 5 | 58 | 5 | 4 | 0.12 | 0.1240 ± 0.0024 |
| C | 20 | 240 | 5 | 3 | 0.10 | 0.1007 ± 0.001 |
| | 5 | 58 | 5 | 4 | 0.10 | 0.1005 ± 0.0005 |
| D | 20 | 240 | 5 | 3 | 0.08 | 0.0776 ± 0.0003 |
| E | 20 | 240 | 5 | 3 | 0.07 | 0.0683 ± 0.0012 |
| F | 5 | 58 | 5 | 4 | 0.06 | 0.0587 ± 0.0016 |
| | 5 | 58 | 5 | 4 | 0.06 | 0.0583 ± 0.0028 |
| | 20 | 240 | 5 | 3 | 0.06 | 0.0612 ± 0.0010 |
| G | 20 | 240 | 5 | 3 | 0.03 | 0.0263 ± 0.0007 |
| | 20 | 240 | 5 | 3 | 0.03 | 0.0273 ± 0.0011 |
| H | 20 | 240 | 5 | 1 | 0.012 | 0.0121 ± 0.0005[a] |
| I | 20 | 240 | 5 | 3 | 0.003 | 0.0048 ± 0.0003 |

[a]Standard deviation in relative activities

The $Eu_xWO_3$ samples were analyzed following exactly the same procedures as in the case of gadolinium. Again, known mixtures were prepared and analyzed. In this case the standard mixture had the ratio Eu/W = 0.5. Despite the relative complexity of the $Eu^{152}$ gamma-ray spectrum, results comparable in accuracy to those obtained for $Gd_xWO_3$ were realized. Table 19 summarizes the results obtained for the analyses of these known mixtures.

Three $Eu_xWO_3$ samples were obtained for analysis. Again, the reported x values were based on the stoichiometric quantities of the constituents used to prepare these samples by the thermal reaction method. Results obtained for these analysis appear in Table 20. Somewhat better agreement between reported and experimentally observed x values is seen in the case of $Eu_xWO_3$ than for the $Gd_xWO_3$ samples. Samples of $Eu_xWO_3$ and $Gd_xWO_3$ were obtained for analysis from Dr. W. Ostertag of the Wright-Patterson Air Force Base.

Table 19. Analysis for Eu in $Eu_2O_3$ - $WO_3$ mixtures

| Sample | Irradiation Time (min) | Time of First Count After Irradiation (min) | Accumulation Time (min) | Number of Spectra Accumulated | x value | |
|---|---|---|---|---|---|---|
| | | | | | Calculated | Observed |
| 1 | 5 | 58 | 5 | 4 | 0.300 | 0.297 ± 0.005 |
| 2 | 5 | 58 | 5 | 4 | 0.200 | 0.196 ± 0.005 |
| 3 | 5 | 58 | 5 | 4 | 0.100 | 0.100 ± 0.004 |
| 4 | 5 | 58 | 5 | 4 | 0.050 | 0.051 ± 0.002 |

Table 20. Analysis for Eu in $Eu_xWO_3$

| Sample | Irradiation Time (min) | Time of First Count After Irradiation (min) | Accumulation Time (min) | Number of Spectra Accumulated | x value | |
|---|---|---|---|---|---|---|
| | | | | | Reported | Observed |
| A | 5 | 58 | 5 | 4 | 0.150 | 0.158 ± 0.006 |
| | 20 | 240 | 5 | 3 | 0.150 | 0.152 ± 0.002 |
| B | 5 | 58 | 5 | 4 | 0.080 | 0.079 ± 0.002 |
| | 20 | 240 | 5 | 3 | 0.080 | 0.080 ± 0.001 |

Table 20. (Continued)

| Sample | Irradiation Time (min) | Time of First Count After Irradiation (min) | Accumulation Time (min) | Number of Spectra Accumulated | x value | |
|---|---|---|---|---|---|---|
| | | | | | Reported | Observed |
| C | 5 | 58 | 5 | 4 | 0.060 | 0.057 ± 0.001 |
| | 20 | 240 | 5 | 3 | 0.060 | 0.057 ± 0.001 |

## RELATIONS BETWEEN X VALUE AND LATTICE PARAMETER

It has been found (21, 22, 24) that the sodium tungsten bronzes crystallize in cubic symmetry for $x \geq 0.4$ and that a linear relation exists between the x value and lattice parameter, $a_o$, for this region. (23) Brown and Banks found this relation to be

$$a_o(\text{Å}) = 0.0819x + 3.7846. \qquad (11)$$

This equation was substantiated by the work of Reuland and Voigt, (48) who determined sodium x values by thermal neutron activation, and found the equation to be

$$a_o(\text{Å}) = 0.0818x + 3.7850. \qquad (12)$$

Tungsten bronzes of lithium (26, 31, 23) and the rare earths (41) also crystallize in cubic symmetry for certain values of x. During the course of this investigation, lattice parameter data for several of the cubic rare earth bronzes were determined from Debye-Scherrer powder photographs by Mr. Howard Shanks. These data were plotted against x values determined by activation analysis for $Gd_xWO_3$ and $U_xWO_3$ samples. A graphical representation of these data is given in Figure 23, together with data representing cubic bronzes of lithium (Shanks) and sodium. (48)

It was not possible to obtain enough data points for $Li_xWO_3$, $Gd_xWO_3$ or $U_xWO_3$ for a suitable least squares analysis. However, it does appear that all graphs of lattice parameter versus x value for the cubic tungsten bronzes have a common intercept. It would seem that the value of this intercept should concur with that observed for $Na_xWO_3$, 3.785. This is dramatically illustrated by the proximity to this value attained by extrapolating the line for $Li_xWO_3$ to $x = 0$. It can be seen that,

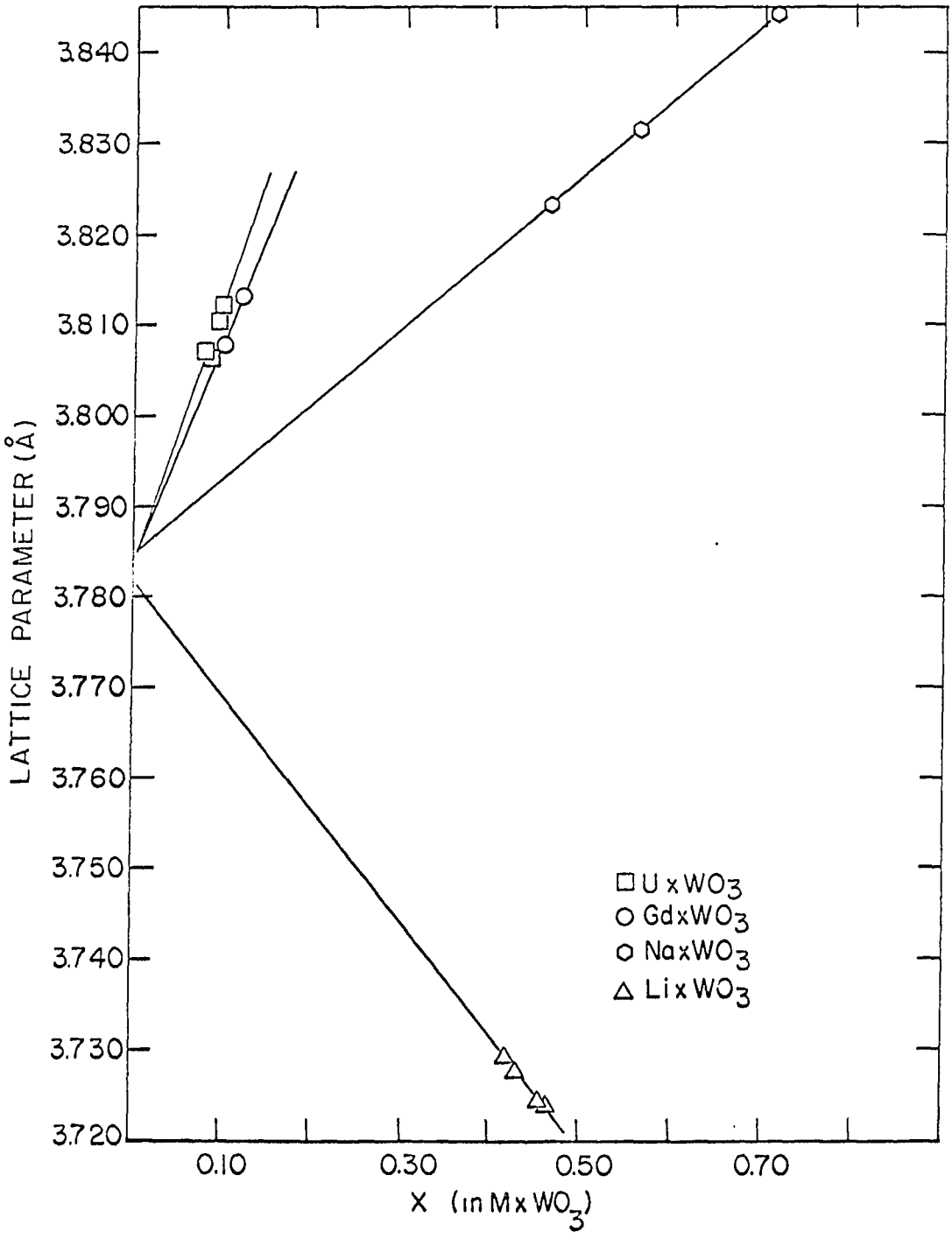


Figure 23. Lattice parameter versus x value for $M_xWO_3$

regardless of slope, all the lines illustrated in Figure 23 intercept the y, or $a_o$, axis at nearly the same point. This point of interception would correspond to the lattice parameter of a theoretical cubic $WO_3$ lattice. No such structure is known to exist for $WO_3$.

## SUMMARY

Three different irradiation techniques were utilized in the non-destructive activation analysis of a number of tungsten bronzes. The x values for tungsten bronzes of eight metals were determined by activation with neutrons and high energy photons.

Following bombardment with thermal neutrons, rubidium, holmium, lanthanum and uranium were determined in their tungsten bronzes by a discriminative analysis of their gamma-ray spectra. The main interference was, in all cases, $W^{187}$. Gamma-ray scintillation spectrometry was used to resolve the photopeaks of interest from $W^{187}$ interference.

Barium was determined in $Ba_xWO_3$ by activation with 14 Mev neutrons. Transfer from irradiation site to counting position was accomplished by means of a pneumatic transfer system which allowed the 2.6 minute $Ba^{137m}$ activity to be counted shortly after irradiation. Interference from $N^{16}$ activity produced by the reaction $O^{16}(n,p)N^{16}$ was eliminated by allowing for the decay of this short lived isotope.

Potassium was determined in $K_xWO_3$ by activation with high energy photons. An internal standard technique was used which compared the activities of $K^{38}/Ta^{185}$ produced in the samples to the ratio produced in standard $K_2WO_5$. Gadolinium and europium were also determined in their tungsten bronzes by photon activation. A computer program was used for these analyses to separate each gamma-ray spectrum into its components. The ratios of activities of $Gd^{159}/W$ and $Eu^{152}/W$ were obtained and compared with ratios obtained for standard samples to determine the x values.

The accuracy of all methods used was determined by analyzing samples of known composition. These mixtures were made to have known metal to

tungsten ratios. In all cases experimentally observed results compared very favorably with the calculated values.

A plot of lattice parameter versus x value was made for the cubic bronzes of sodium, lithium, gadolinium and europium. On the basis of these graphs it appears that all linear relations between x value and lattice parameter for cubic tungsten bronzes may have a common intercept when extrapolated to $x = 0$.

This investigation has shown that many tungsten bronzes may be determined nondestructively and without regard to structure by activation analysis. It has also indicated a relationship between lattice parameter and x value which may be common to all cubic tungsten bronzes.

LITERATURE CITED


1. von Hevesy, G. and Levi, H. Kgl. Danske Videnskab. Selskab, Mat.-fys. Medd. 14, No. 5, 1 (1936).

2. Seaborg, G. T. and Livengood, J. J. J. Am. Chem. Soc. 60, 1784 (1938).

3. von Halban, H., Joliot, F. and Kowarski, L. Nature 143, 680 (1939).

4. Meinke, W. W. Anal. Chem. 28, 736 (1956).

5. Meinke, W. W. Anal. Chem. 30, 686 (1958).

6. Meinke, W. W. Anal. Chem. 32, 104R (1960).

7. Leddicotte, G. W. Anal. Chem. 34, 143R (1962).

8. Leddicotte, G. W. Anal. Chem. 36, 419R (1964).

9. Lyon, W. S., Ricci, E. and Ross, H. H. Anal. Chem. 38, 521R (1966).

10. Koch, R. C. Activation Analysis Handbook. New York, N. Y., Academic Press, Inc. (1960).

11. Lyon, W. S., Jr., ed. Guide to Activation Analysis. Princeton, N. J., D. Van Nostrand Co., Inc. (1964).

12. Crouthamel, C. E. Applied Gamma-Ray Spectrometry. New York, N. Y., Pergamon Press, Inc. 1960.

13. Jenkins, E. N. and Smales, A. A. Quart. Revs. (London) 10, 83 (1956).

14. Atkins, D. H. F. and Smales, A. A. Advances in Inorganic Chemistry and Radiochemistry 1, 315 (1959).

15. Bowen, H. J. M. and Gibbons, D. Radioactivation Analysis. London, England, Oxford University Press (1963).

16. Lewis, W. B. Nucleonics 13, No. 10, 82 (1955).

17. Moteff, J. and Beever, E. R. Selected Topics in Radiation Dosimetry, International Atomic Energy Agency, Austria (1961).

18. Kramer, H. H. and Wahl, W. H. Nuc. Sci. and Eng. 22, 373 (1965).

19. Wohler, F. Ann. chim. et phys. Ser. 2, 29, 43 (1823).

20. Wohler, F. Pogg. Ann. 2, 350 (1824).

21. Hagg, G. Z. Nature 135, 874 (1935).

22. Hagg, G. Z. Z. physik. Chem. B29, 192 (1935).

23. Brown, B. W. and Banks, E. J. Am. Chem. Soc. 76, 963 (1954).

24. de Jong, W. F. Z. Krist. 81, 314 (1932).

25. Magneli, A. Arkiv Kemi 1, 269 (1949).

26. Magneli, A. and Blomberg, B. Acta Chem. Scand. 5, 372 (1951).

27. Straumanis, M. E. J. Am. Chem. Soc. 71, 679 (1949).

28. Brimm, E. O., Brantley, J. C., Lorenz, J. H. and Jellinek, M. H. J. Am. Chem. Soc. 73, 5427 (1951).

29. Hallopeau, L. A. Ann. chim. phys. 19, 117 (1900).

30. Brunner, O. Beitrage zur Kenntnis der Wolframbronzen. Unpublished Ph.D. thesis. Zurich, Switzerland, Library, University of Zurich. (1903).

31. Magneli, A. and Nilsson, R. Acta Chem. Scand. 4, 398 (1950).

32. Straumanis, M. E. and Hsu, S. S. J. Am. Chem. Soc. 72, 4027 (1950).

33. Magneli, A. Acta Chem. Scand. 1, 315 (1953).

34. Sienko, M. J. and Morehouse, S. M. Inorg. Chem. 2, 485 (1963).

35. Laurent, A. Ann. Chim, Phys. 67, No. 2, 215 (1838).

36. von Knorre, G. J. Prakt. Chem. 27, No. 2, 49 (1883).

37. Schaefer, E. Z. anorg. u. allgem. Chem. 38, 158 (1904).

38. Conroy, L. E. and Yokokawa, T. Inorg. Chem. 4, 994 (1950).

39. Sweedler, A. R., Hulm, J. K., Matthias, B. T. and Geballe, T. H. Physics Letters 19, No. 2, 82 (1965).

40. Ostertag, W. Inorg. Chem. 5, 758 (1966).

41. Collins, C. V. and Ostertag, W. J. Am. Chem. Soc. 88, 3171 (1966).

42. Conroy, L. E. and Sienko, M. J. J. Am. Chem. Soc. 79, 4048 (1957).

43. Sienko, M. J. and Mazumder, B. R. J. Am. Chem. Soc. 82, 3508 (1960).

44. Sienko, M. J. J. Am. Chem. Soc. 81, 5556 (1959).

45. Spitzin, V. and Kaschtanoff, L. Z. anorg. u. allgem. Chem. 157, 141 (1926).

46. Spitzin, V. and Kaschtanoff, L. Z. anal. Chem. 75, 440 (1928).

47. Raby, B. A. and Banks, C. V. Anal. Chem. 36, 1106 (1964).

48. Reuland, R. J. and Voigt, A. F. Anal. Chem. 35, 1263 (1963).

49. Soltys, M. N. and Morrison, G. H. Anal. Chem. 36, 293 (1964).

50. Nuclear Data Sheets. Washington, D. C., National Academy of Sciences--National Research Council. (1958-1962).

51. Nuclear Data Sheets. Sec. B. Washington, D. C., National Academy of Sciences--National Research Council. (1964)

52. Gillespie, A. S., Jr. and Hill, W. W. Nucleonics 19, No. 11, 170 (1961).

53. Okada, M. Nucleonics 22, No. 8, 110 (1964).

54. Hammer, C. L. and Bureau, A. J. Rev. Sci. Instr. 32, 93 (1961).

ACKNOWLEDGMENTS

The author expresses her sincere gratitude to Dr. Adolf Voigt for his help and encouragement during the course of this investigation and through her years of training at Iowa State University.

Thanks are also due to Dr. Alfred Bureau of the Iowa State University Synchrotron staff, to members of the staffs of the UTR-10 Reactor and of the Ames Laboratory Research reactor, and to members of Radiochemistry Group I, particularly Messrs. Peter Korthoven and Wayne Stensland.

The author also wishes to acknowledge Mr. Howard Shanks and Dr. Werner Ostertag for providing the tungsten bronze samples.